A MICROMACHINED PRESSURE SENSOR

A THESIS SUBMITTED TO

THE GRADUATE SCHOOL OF ENGINEERING AND SCIENCE

OF BILKENT UNIVERSITY

IN PARTIAL FULFILLMENT OF THE REQUIREMENTS FOR

THE DEGREE OF

MASTER OF SCIENCE

IN

ELECTRICAL AND ELECTRONICS ENGINEERING

By

Hasan Karaca

September 2017

A Micromachined Pressure Sensor

By Hasan Karaca

September 2017

We certify that we have read this thesis and that in our opinion it is fully adequate, in scope and in quality, as a thesis for the degree of Master of Science.

Abdullah Atalar (Advisor)

Hayrettin Köymen

Barış Bayram

Approved for the Graduate School of Engineering and Science:

Ezhan Karasan
Director of the Graduate School

ABSTRACT

A MICROMACHINED PRESSURE SENSOR

Hasan Karaca
M.Sc. in Electrical and Electronics Engineering
Advisor: Abdullah Atalar
September 2017

Capacitive Micromachined Ultrasonic Transducer (CMUT) is a microelectromechanical device that is basically formed by a moving top electrode, a stable bottom electrode and a gap in between. In spite of its this simple mass-spring construction, CMUT is a nonlinear device and its working principles have been formulated. According to these studies, the top electrode can be set in motion by the applied pressure on it and by depending on the amount of that pressure, the resonant frequency of the CMUT can be altered. Therefore, it is possible to use CMUT to obtain a pressure sensor. In this respect, what we have to do is keep tracking of its resonant frequency to deduce the pressure. The most effective way of doing it, on the other hand, is using an oscillator circuit which also provides us the capability of tracking the resonant frequency in real time. Also, to design an integrated circuit that works with the CMUT, the best way is utilizing a Colpitts oscillator. In this thesis, we design a pressure sensor with CMUT based Colpitts oscillator.

In order to achieve our design, first of all, we examine the small signal equivalent circuit model of an uncollapsed mode CMUT and investigate the related analytical equations that models the behavior of it. To simplify the equations, we liken the small signal equivalent circuit model to a crystal oscillator by making necessary transformations. After that, we investigate the "feedback system approach" and "negative resistance concept" methods that help us to analyze the oscillator circuits; and we determine the Colpitts oscillator circuit as the oscillator circuit part of our device. We evaluate the CMUT based Colpitts oscillator circuit and derive the limitations on the circuit parameters for achieving a power efficient device. In addition to that, we discuss the dc biasing of the oscillator circuit that does not cause any loading effect on the oscillator circuit and design a ring oscillator and a charge pump circuit which help us to obtain bias voltage on the CMUT. Finally, we calculate the sensitivity (in Hz/Pa) and the temperature sensitivity of a CMUT in addition to the Quality factor of our circuit; and by being based on these calculations, we obtain the optimum CMUT parameters for the best available sensitivity and conclude the design.

At the end, we design a CMUT based Colpitts oscillator that works as a pressure sensor which measures pressure between zero atm and one atm with sensitivity of 14.6 Hz/Pa at 1 atm. The selected CMUT parameters, on the other hand, for the radius of the CMUT cell, the gap height of the CMUT cell, the thickness of the insulator layer and the thickness of the top plate are 44 μm, 100 nm, 100 nm and 3 μm respectively. The Quality factor of the circuit is 5 and the inherent Quality factor of the CMUT is 432.

Keywords: CMUT, Capacitive Micromachined Ultrasonic Transducer, uncollapsed mode, Oscillator, Colpitts Oscillator, Pressure Sensor.

ÖZET

MİKROİŞLENMİŞ BASINÇ SENSÖRÜ

Hasan Karaca
Elektrik ve Elektronik Mühendisliği, Yüksek Lisans
Tez Danışmanı: Abdullah Atalar
Eylül 2017

Kapasitif mikroişlenmiş ultrasonik çevirici (CMUT), basitçe, aralarında boşluk bulunan hareket eden bir üst elektrot ile sabit bir alt elektrottan oluşan mikroelektromekanik bir cihazdır. Bu sade kütle-yay yapısına rağmen, CMUT lineer olmayan bir cihazdır ve çalışma prensipleri son zamanlarda formüle edilmiştir. Bu çalışmalara göre, üzerine uygulanan basınç ile üst elektrot hareket ettirilebilir ve basıncın miktarına göre de CMUT'ın rezonans frekansı değiştirilebilir. Dolayısıyla, CMUT'ı bir basınç sensörü elde etmek için kullanmak mümkündür. Bu açıdan, basıncı ortaya çıkarmak için yapmamız gereken şey CMUT'ın rezonans frekansını takip etmektir. Bunun en etkin yolu ise, bize CMUT'ın rezonans frekansını gerçek zamanlı takip etme kabiliyetini de sağlayan osilatör kullanımıdır. Ayrıca, CMUT ile çalışan entegre devreler dizaynı içinse en iyi yol Colpitts osilatörden yararlanmaktr. Bu tezde biz entegre devre (IC) düzeyinde bir dizayn hedeflediğimizden, CMUT tabanlı Colpitts osilatör ile bir basınç sensörü dizayn ediyoruz.

Dizaynımızı elde etmek için, ilk önce, çökmemiş modda CMUT'ın küçük sinyal eşdeğer devre modelini inceliyor ve davranışını modelleyen ilgili analitik denklemleri tahkik ediyoruz. Daha sonra, denklemleri sadeleştirmek için küçük sinyal eşdeğer devre modelini gerekli dönüşümleri yaparak kristal osilatöre benzetiyoruz. Bundan sonra ise, osilatörleri analiz etmemize yardım eden "geri-besleme sistemi yaklaşımı" ve "negatif direnç kavramı" metodlarını inceliyor ve Colpitts osilatörünü cihazımızın osilatör kısmı olarak tespit ediyoruz. Sonra da, bu metodlara dayanarak CMUT tabanlı Colpitts osilatörümüzü değerlendirip, güç açısından verimli bir cihaz elde etmemiz için devre parametreleri üzerinde bulunan sınırlamaları ortaya çıkartıyoruz. Colpitts osilatörle ilgili olarak ayrıca, osilatör üzerinde hiçbir yükleme etkisine sebep olmayan dc bayaslamayı müzakere ediyor ve CMUT üzerindeki bayas voltajını elde etmemize yardım eden bir halka osilatörü ve bir de şarj pompası devresi dizayn ediyoruz. Nihayet, devremizin kalite

faktörünün yanısıra, bir CMUT için duyarlılık (Hz/Pa) ve sıcaklık duyarlılığını hesaplıyor ve elde edilebilir en iyi duyarlılık değeri için en uygun CMUT parametrelerini elde ediyor ve dizaynı sonuçlandırıyoruz.

En sonunda, sıfır atm ve bir atm arasındaki basıncı 1 atmde 14.6 Hz/Pa duyarlılık ile ölçen ve basınç sensörü olarak çalışan CMUT tabanlı Colpitts osilatörü dizayn ediyoruz. Seçilmiş CMUT parametreleri ise CMUT hücresinin yarıçapı, CMUT hücresisin boşluk yüksekliği, yalıtıcı tabakanın kalınlığı ve üst plakanın kalınlığı için sırayla 44 μm, 100 nm, 100 nm ve 3 μm. Devrenin ve CMUT'ın içsel kalite faktörleri ise 5 ve 432.

Anahtar sözcükler: CMUT, Kapasitif Mikroişlenmiş Ultrasonik Çevirici, çökmemiş mod, Osilatör, Colpitts Osilatör, Basınç Sensörü.

Acknowledgement

I would like to express my deepest gratitude to my advisor Prof. Dr. Abdullah Atalar for his contribution and guidance throughout the development of this thesis.

I would like to express my sincerest gratitude to Dr. Mehmet Yılmaz for teaching and helping me about CMUT mask design with Tanner L-Edit and CMUT production both theoretically and practically.

I would like to thank Murat Güre for teaching and helping me about usage of VAKSİS PECVD to obtain low stress silicon nitride.

I am grateful to Prof. Dr. Orhan Arıkan for his support and contributions. Without him, this thesis even cannot be possible.

My appreciation to Mürüvet Parlakay and Yüksel Angelidu for making our lives easier in both the department and the university.

A special thank to my friend Cem Bülbül for his helps in Cadence and special thanks to my friends Muhittin Taşçı, Yasin Kumru and Murat Güngen.

Finally, I would like to thank my mom Durdu, my father Bilal, my sister Elif and my brother Yusuf Emir for their love and endless support.

I dedicate this thesis to world peace and to animals under threat of extinction.

Contents

1 Introduction **1**

2 CMUT **4**

2.1 CMUT Small Signal Equivalent Circuit Model and Analytical Equations 4

2.2 Simplification for the CMUT Small Signal Equivalent Circuit Model 8

3 OSCILLATOR **11**

3.1 Oscillator 11

3.1.1 Feedback System Approach 12

3.1.2 Negative Resistance Concept 13

3.2 Oscillator Selection Criteria 14

4 CIRCUIT DESIGN **16**

4.1 CMUT based Colpitts Oscillator 16

4.2 Analysis of the Circuit based on Feedback System Approach . . . 20

4.3 DC Biasing of the Colpitts Oscillator 23

4.4 Ring Oscillator 26

4.5 Charge Pump Circuit 27

4.6 Final Design 27

5 OPTIMUM CMUT **34**

5.1 Calculation of Sensitivity 34

5.2 Calculation of the Quality Factor 39

5.3 Temperature (T) Sensitivity 41

5.4 Selection of the Optimum CMUT 42

6 CONCLUSION **46**

A CMUT MATLAB Code **53**

A.1 CMUT.m 53

A.2 gFunc2.m 58

A.3 gFirstDerivativeFunc2.m 59

A.4 gSecondDerivativeFunc2.m 59

List of Figures

2.1 Geometrical parameters of a circular capacitive micromachined ultrasound transducer (CMUT) in two dimensional view [1, 2, 3] . . 5

2.2 Small signal equivalent circuit model for a capacitive micromachined ultrasound transducer (CMUT) [1, 2, 3] 5

2.3 Simplified CMUT model [4] 8

2.4 Reactance versus frequency relation of a CMUT [5] 10

3.1 Sinusoidal oscillator block diagram 12

3.2 Negative resistance oscillator 13

3.3 Illustration of CMUT between its series and parallel resonant frequencies and representation of Colpitts oscillator 15

4.1 CMUT and Colpitts Oscillator 17

4.2 Small signal equivalent circuit for Colpitts oscillator 18

4.3 The loop in the CMUT based Colpitts oscillator circuit 21

4.4 DC bias circuit with the Colpitts oscillator 25

4.5 Oscillating signal approximately between 5 V and 0 V 25

4.6 Design for the three stage ring oscillator [6] 28

4.7 Oscillating signal at each stage of the three stage ring oscillator . 28

4.8 Voltage quadrupler circuit [7] 29

4.9 Simulation results for the charge pump circuit and voltages on each net 29

4.10 Final design for the CMUT based Colpitts oscillator 30

4.11 Layout of the CMUT based Colpitts oscillator 31

4.12 Two dimensional view representation of the diodes 32

4.13 Two dimensional view representation of a NMOS transistor 32

4.14 Two dimensional view representation of a PMOS transistor 33

4.15 Two dimensional view representation of the resistor 33

5.1 $\frac{df_0}{dP_0}$ versus $\frac{F_{Pb}}{F_{Pg}}$ for different values of t_m 39

5.2 Overall CMUT based Colpitts oscillator in small signal 40

5.3 Overall CMUT based Colpitts oscillator in small signal with new parameters 41

5.4 t_{ge} versus $\frac{F_{Pb}}{F_{Pg}}$ for different values of t_m 43

5.5 R_{CMUT} versus $\frac{F_{Pb}}{F_{Pg}}$ for different values of t_m 44

List of Tables

1.1 Comparison of our device with other pressure sensors 3

5.1 Optimum parameters for the CMUT 45

Chapter 1

Introduction

Capacitive Micromachined Ultrasonic Ttransducer (CMUT) is a microelectromechanical structure that consists of two electrodes and a vacuum gap in between. Top electrode stays within a suspended membrane and bottom electrode lies on the substrate. By depending on the formed electric field or any other mechanical disturbance among electrodes, membrane is deflected by resulting in a change in the value of capacitance.

CMUT has recently been commercialized for medical ultrasound imaging purposes [8, 9]. In addition to that, it has several other applications such as acoustic signal source [10, 11], chemical gas sensor [12, 13, 14, 15, 16, 17] and pressure sensor [18, 19].

CMUT is a nonlinear device and its properties are affected by the materials used in membrane formation, geometry of the device, pressure around, voltage on it and surrounding environment such as liquid or air. Due to its complicated structure, many efforts have been performed to accurately simulate the device. Some researchers tried to model it by basing on the experimental observations [12, 14, 15, 17] and some researchers benefited from energy equivalent method [20]. Recently, an effort have been expended on this subject and the analytical expressions for a circular CMUT membrane profile was derived for both collapsed and uncollapsed modes [21, 22]. In this work, SPICE is used as circuit simulator and finite element method (FEM) is utilized to test the accuracy of the model. With these simulations, the model achieved to predict CMUT with an accuracy rate of better than 3%. Oğuz developed a circuit theory based CMUT model for uncollapsed mode [1, 23] and Aydoğdu achieved a lumped element model for collapsed mode [24, 25]. An explanatory study was also conducted [2, 3] for the nonlinear lumped element circuit model of a circular uncollapsed mode CMUT cell.

In this thesis, we have designed a pressure sensor with CMUT based oscillator at integrated circuit design level. The CMUT is in uncollapsed mode and developed in MATLAB by combining proper equations from references [1, 2, 3, 23]. For oscillator design, we have benefited from Razavi's book: "Design of Analog CMOS Integrated circuits" [6] and developed the circuit with CADENCE. Since we have planned to combine CMUT and oscillator circuit with wire bonding method, we used Colpitts oscillator among any other design models. Therefore, at oscillation frequency CMUT behaved like a lossy inductor and provided us with connecting one side of CMUT to its bias voltage while other side is connected to the oscillation circuit by wire bonding. In addition to that, with this design, we were able to develop CMUT and oscillator circuit separately. The most important parameters during the design process were breakdown voltage of MOSFETs, practicability of CMUT with desired geometry parameters and sensitivity of circuit against pressure. We are designing a pressure sensor; therefore, against the change in pressure, we need to keep change of oscillation frequency in the structure at maximum to have best sensitivity. Our device has a *sensitivity* of 14.6 Hz/Pa at 1 atm. In this respect, it has a comparable sensitivity performance with respect to other pressure sensors as indicated in Table 1.1 [18, 19, 26, 27, 28].

This thesis consists of six chapters. In chapter two, we investigate the small signal equivalent circuit model of an uncollapsed mode CMUT and examine the related analytical equations that models the behavior of it. Also, in the same chapter, we liken the CMUT to a crystal oscillator for simplification purposes. In chapter three, we discuss the analytical methods of the "feedback system approach" and the "negative resistance concept" that help us to comprehend

Comparison of our device with other pressure sensors			
Devices	Sensitivity	Pressure range	DC bias voltage
Our device	14.6 Hz/Pa	0-1 atm	12.5 V
Li, 2015 [18]	68 Hz/Pa	0-100 Pa	16 V
Li, 2014 [19]	30 Hz/Pa	0-120 Pa	42.75 V
Southworth, 2009 [26]	15 Hz/Pa	0-1 atm	-
Stedman, 2016 [27]	0.06 Hz/Pa	0-1 atm	-
Fonseca, 2002 [28]	1.41 Hz/Pa	0-7 atm	-

Table 1.1: Comparison of our device with other pressure sensors

whether an oscillator circuit works or not. Then, by depending on the certain criteria, we select the Colpitts oscillator circuit as the oscillator part of the design. In chapter four, we design a Colpitts oscillator circuit; and then, by depending on the analytical methods above, we derive the restrictions on the circuit parameters to achieve a power efficient device. In this chapter, we discuss the dc biasing of the oscillator circuit that does not cause any loading effect on the oscillator circuit and design a ring oscillator and a charge pump circuit to obtain the bias voltage on the CMUT. In chapter five, we calculate the *sensitivity* (in Hz/Pa) and the temperature sensitivity of a CMUT in addition to the Quality factor of our circuit. Then, by depending on these calculations, we choose the optimum CMUT. Finally, in chapter six, we conclude our study.

Chapter 2

CMUT

In this chapter, we investigate the small signal equivalent circuit model and the related analytical equations which models the behavior of a CMUT in uncollapsed mode. The equations are taken or derived from previous studies [1, 2, 3, 23].

2.1 CMUT Small Signal Equivalent Circuit Model and Analytical Equations

The geometrical parameters of a circular capacitive micromachined ultrasound transducer (CMUT) in two dimensional view is shown in Fig. 2.1. In the figure, aperture radius, radial position, displacement profile, gap height of the cell, thickness of the insulator layer and thickness of the top plate are symbolized as a, r, $x(r)$, t_g, t_i and t_m, respectively.

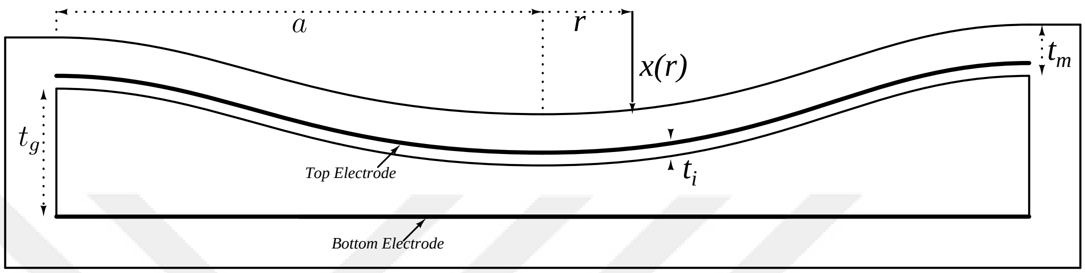

Figure 2.1: Geometrical parameters of a circular capacitive micromachined ultrasound transducer (CMUT) in two dimensional view [1, 2, 3]

The corresponding small signal equivalent circuit model for a circular uncollpased mode CMUT can be observed in Fig. 2.2. In this figure, the capacitance between electrodes including impact of the top plate deflection, the turns ratio of electromechanical transformer, the effect of spring softening factor, the compliance of the top plate, the effective mass of the top plate and the radiation impedance are represented by C_{0d}, n_R, C_{RS}, C_{Rm}, L_{Rm} and Z_{RR}, respectively.

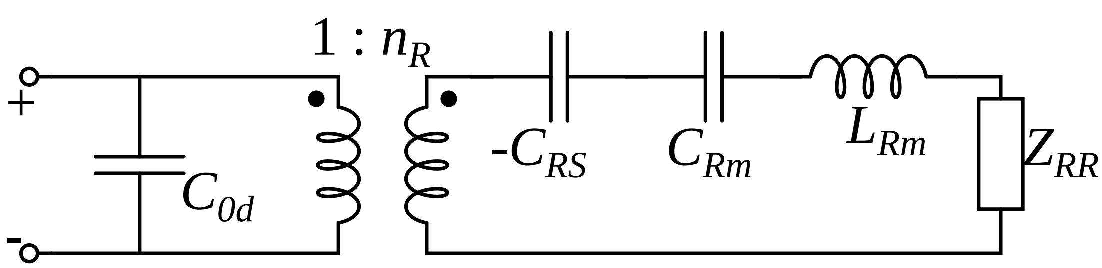

Figure 2.2: Small signal equivalent circuit model for a capacitive micromachined ultrasound transducer (CMUT) [1, 2, 3]

The circuit parameter C_{0d} arises due to capacitance between top and bottom electrode structures, and effect of deflection at the top plate is also included in it. Thus, its value is calculated as

$$C_{0d} = C_0 \; g\left(\frac{X_P}{t_{ge}}\right) \tag{2.1}$$

where C_0 is the capacitance between top and bottom electrodes, and it is found as

$$C_0 = \epsilon_0 \, \frac{\pi \, a^2}{t_{ge}} \tag{2.2}$$

where a is the radius of a circular CMUT cell and t_{ge} in both Eqs. 2.1 and 2.2 is the effective gap height. The value of t_{ge} is

$$t_{ge} = t_g \, + \frac{t_i}{\epsilon_r} \tag{2.3}$$

where t_g is the gap height of a CMUT cell whereas t_i and ϵ_r are thickness and relative permitivity of the insulator, respectively.

The function $g()$ in Eq. 2.1 adds the effect of top plate deflection to the capacitance and it is given as

$$g(u) = \frac{\tanh^{-1}(\sqrt{u})}{\sqrt{u}} \tag{2.4}$$

The last unknown term in Eq. 2.1, X_P is the deflection of the top plate at the center of it and it is derived from the equation

$$\frac{3X_P}{t_{ge}} - \frac{5\pi a^2 P_0 C_{Rm}}{t_{ge}} - 2g'\left(\frac{X_P}{t_{ge}}\right)\left(\frac{V_{DC}}{V_r}\right)^2 = 0 \tag{2.5}$$

where P_0 is the ambient pressure, V_{DC} is the DC bias voltage on CMUT and V_r is the collapse voltage in the case of no ambient pressure. The calculation of V_r is also as follows

$$V_r = 8\frac{t_m^{3/2} t_{ge}^{3/2}}{a^2}\sqrt{\frac{Y_0}{27\epsilon_0(1-\sigma^2)}} \tag{2.6}$$

where t_m, Y_0 and σ are thickness, Young's modulus and Poisson's ratio of the top plate, respectively. Another unknown C_{Rm} in Eq. 2.5 is also a circuit parameter in the small signal equivalent model and stems from the compliance of the top plate [1, 2, 29]. Its value decreases as the top plate gets stiffer [1] and it is obtained from the equation of

$$C_{Rm} = \frac{9}{5}\frac{(1-\sigma^2)a^2}{16\pi Y_0 t_m^3} \tag{2.7}$$

Finally, the function $g'()$ in Eq. 2.5 is given as

$$g'(u) = \frac{1}{2u}\left(\frac{1}{1-u} - \frac{\tanh^{-1}(\sqrt{u})}{\sqrt{u}}\right) \tag{2.8}$$

Another circuit parameter in Fig. 2.2, n_R is the turns ratio of the electromechanical transformer and it is found from the formula of

$$n_R = \sqrt{5}\frac{C_0 V_{DC}}{t_{ge}} g'\left(\frac{X_P}{t_{ge}}\right) \tag{2.9}$$

C_{RS} arises from the spring-softening effect [1, 2, 29] and it behaves in a way to reduce the mechanical stiffness of the top plate. That is why C_{RS} is shown with a negative sign in the small signal equivalent circuit model. The value of C_{RS} is calculated as in the following equation

$$C_{RS} = \frac{2t_{ge}^2}{5C_0 V_{DC}^2 g''\left(\frac{X_P}{t_{ge}}\right)} \tag{2.10}$$

where

$$g''(u) = \frac{1}{2u}\left(\frac{1}{(1-u)^2} - 3g'(u)\right) \tag{2.11}$$

The circuit parameter L_{Rm} in the small signal equivalent circuit model comes due to mass of the top plate and it is found as

$$L_{Rm} = \rho\pi a^2 t_m \tag{2.12}$$

where ρ is density of the top plate.

As it is explained in [1] and [30], radiation impedance for a CMUT, Z_{RR}, is the ratio of total radiated power from acoustic terminals to the square of the absolute value of the CMUT's nonzero reference velocity. The related formula is given as

$$Z_R = \frac{2\pi\int_0^a P(r)v^*(r)r dr}{V_i V_i^*} = \frac{P_{TOTAL}}{|V_i|^2} \tag{2.13}$$

When the rms value of the velocity is selected as the value of the velocity, the formula becomes

$$Z_{RR} = \pi a^2 \rho_0 c\left(1 - \frac{20}{(ka)^9}\big[F_1(2ka) + jF_2(2ka)\big]\right) \tag{2.14}$$

where ρ_0 and c are density of the immersion medium and speed of sound in the immersion medium, respectively. In addition to that, k is the wave number and

$$F_1(y) = \big(y^4 - 91y^2 + 504\big)J_1(y) + 14y(y^2-18)J_0(y) \\ - y^5/16 - y^7/768 \tag{2.15}$$

and

$$F_2(y) = -\big(y^4 - 91y^2 + 504\big)H_1(y) - 14y(y^2 - 18)H_0(y) + 14y^4/15\pi - 168y^2/\pi \tag{2.16}$$

where J_n is the nth order Bessel function and H_n is the nth order Struve function. Radiation impedance represents mechanical power lost to the immersium medium [13, 17, 31, 32].

2.2 Simplification for the CMUT Small Signal Equivalent Circuit Model

In order to make calculations easier, the small signal equivalent circuit model in Fig. 2.2 can be simplified by transforming parameters at the secondary side of the electromechanical transformer to the primary side. The simplified model can be observed in Fig. 2.3.

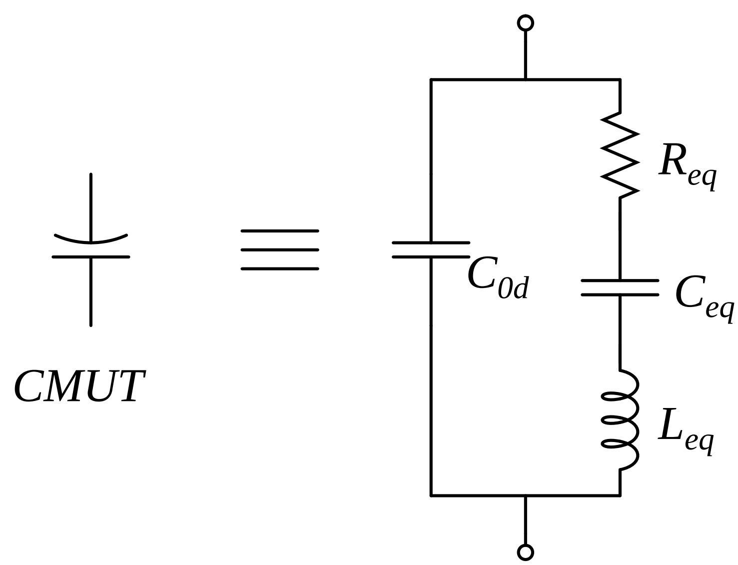

Figure 2.3: Simplified CMUT model [4]

In there, C_{0d} is the same parameter as in small signal equivalent circuit and

$$R_{eq} = \frac{1}{n_R^2}\,\mathbb{R}\mathrm{e}\{Z_{RR}\} \tag{2.17}$$

$$C_{eq} = n_R^2\left(\frac{(-C_{RS})(C_{Rm})}{(-C_{RS})+(C_{Rm})}\right) \tag{2.18}$$

$$L_{eq} = \frac{1}{n_R^2}\left(L_{Rm} + \mathbb{I}\mathrm{m}\{Z_{RR}\}\right) \tag{2.19}$$

where $\mathbb{I}\mathrm{m}\{Z_{RR}\}$ is negligible compared to L_{Rm}.

In addition to that, equivalent impedance of CMUT (Z_{CMUT}) is

$$Z_{CMUT} = \frac{\left(R_{eq} + j\omega L_{eq} + \frac{1}{j\omega C_{eq}}\right)\left(\frac{1}{j\omega C_{0d}}\right)}{\left(R_{eq} + j\omega L_{eq} + \frac{1}{j\omega}\left(\frac{1}{C_{eq}} + \frac{1}{C_{0d}}\right)\right)} \tag{2.20}$$

and Quality Factor (Q), series resonant frequency (f_s) and parallel resonant frequency (f_p) are

$$Q = \frac{\omega L_{eq}}{R_{eq}} \tag{2.21}$$

$$f_s = \frac{1}{2\pi\sqrt{L_{eq}C_{eq}}} \tag{2.22}$$

$$f_p = \frac{1}{2\pi\sqrt{L_{eq}\left(\frac{C_{eq}C_{0d}}{C_{eq}+C_{0d}}\right)}} \tag{2.23}$$

In the series resonant frequency, L_{eq} resonates with C_{eq} and results in a minimum impedance value. On the other hand, in the parallel resonant frequency, L_{eq} resonates with $\left(\frac{1}{C_{eq}} + \frac{1}{C_{0d}}\right)^{-1}$.

The simplified CMUT small signal equivalent circuit looks like the equivalent circuit of a crystal. Therefore, their reactance versus frequency relation are also similar to each other. The relation is shown in Fig. 2.4.

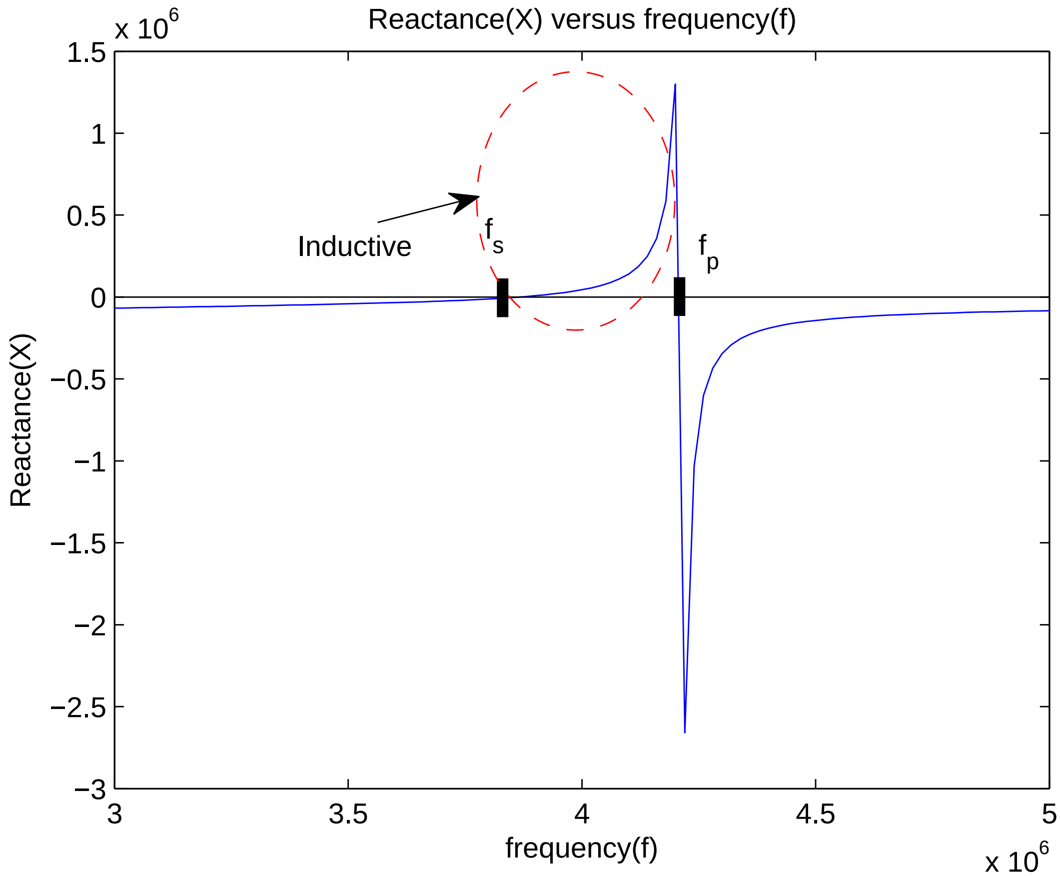

Figure 2.4: Reactance versus frequency relation of a CMUT [5]

As it is indicated in the Fig. 2.4, the reactance is only inductive between series and parallel resonant frequencies. Hence, CMUT can be used in place of the inductor in a Colpitts oscillator in this frequency interval.

Chapter 3

OSCILLATOR

The resonant frequency of the CMUT can be obtained via an oscillator circuit so that we can track the resonant frequency in real time. In this chapter, we describe the oscillator circuit.

3.1 Oscillator

Basically, an oscillator transforms DC power into an AC waveform. Although many distinct signal forms such as rectangular, triangular and sawtooth can be produced with oscillators, they are mostly used to obtain sinusoidal outputs.

There exist actually two distinct analytical methods for the analysis of the oscillators: feedback system approach and negative resistance concept. In the first method, we make a closed loop analysis and by being based on some certain criteria we decide whether an oscillator circuit oscillates or not. In the second method, however, we benefit from the "negative resistance" phenomenon and use the oscillator circuit as the source of negative resistance.

3.1.1 Feedback System Approach

Conceptually, how a sinusoidal oscillator operates can be portrayed with a linear feedback circuit as in Fig. 3.1.

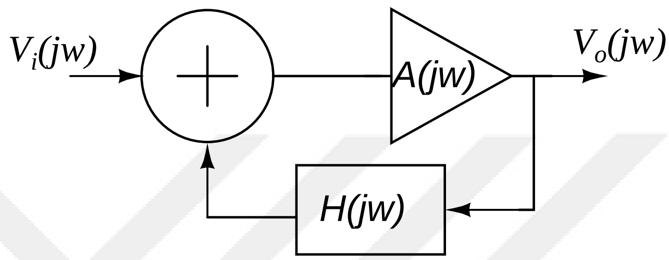

Figure 3.1: Sinusoidal oscillator block diagram

In this figure, an amplifier which has a voltage gain $A(jw)$ gives an output voltage $V_o(jw)$. Then, through a feedback network which has a frequency dependent transfer function $H(jw)$, this voltage passes and merges with the input $V_i(jw)$. Therefore, the output voltage can be written in terms of input voltage as

$$V_o(jw) = \frac{A(jw)}{1 - A(jw)H(jw)} V_i(jw) \tag{3.1}$$

In Eq. 3.1, at a particular frequency, if the denominator becomes zero, a nonzero output voltage can be achieved for a zero input voltage. Hence, it forms an oscillator. This condition is also known as "Barkhausen criteria". Barkhausen criteria says that for an oscillator circuit to oscillate at a certain frequency w_o, loop gain should be equal to unity and phase must be an integer multiple of 2π. These conditions are also formulated as

$$|A(jw_o)H(jw_o)| = 1 \tag{3.2}$$

$$\angle\big(A(jw_o)H(jw_o)\big) = 2n\pi \quad \text{where} \quad n \in 0, 1, 2, ... \tag{3.3}$$

These conditions are actually necessary but not sufficient [33]. In the case of existence of process and temperature variations, oscillation may not start. Therefore, so as to ensure oscillation, in practice, loop gain should be at least two or three times higher than the value in criteria.

3.1.2 Negative Resistance Concept

Negative resistance is a behavior that voltage and current are inversely proportional to each other. In the case of the negative resistance for instance, an increase in voltage value results in a decrease in the current. Negative resistance can be obtained by using passive components like tunnel diodes and active devices like transistors.

Now, consider the circuit in Fig. 3.2. In there, R_L and X_L represents the circuit with positive resistance whereas R_a and X_a symbolizes the active device with negative resistance.

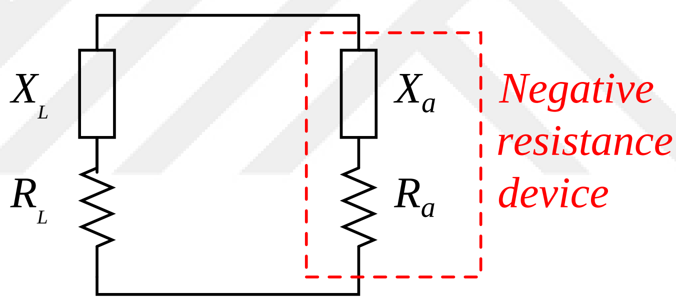

Figure 3.2: Negative resistance oscillator

For this circuit to oscillate, active circuit resistance (R_a) not only should be negative but also its magnitude must be greater than the magnitude of R_L. In addition to that, the reactance of the active circuit should be such that, these two reactances will cancel each other. These conditions can be formulated as

$$|R_a| > R_L \tag{3.4}$$

and

$$-X_a = X_L \tag{3.5}$$

Once these equations are satisfied at a certain frequency, the net resistance of the overall system will be negative. It means that the circuit is acting like a source of energy at that particular frequency. Therefore, when the system operates at a frequency at which overall resistance is negative and whole reactance is zero, we observe oscillations.

In practice, as the oscillator power increases, R_a becomes less negative. Thus, in order to ensure oscillation, a practical value of

$$R_L \approx \frac{-R_a}{3} \tag{3.6}$$

is typically used.

3.2 Oscillator Selection Criteria

There are many kind of oscillators to use for different purposes. In this thesis, however, we will not discuss the types of oscillators in detail. Therefore, under this title, we will just give information about our selection criteria and among many types of oscillator designs, we will choose the one that meets our requirements, directly.

In our system, we want to the design oscillator circuit and CMUT separately and then connect them with wire bonding. In addition to that, we want one side of CMUT to be connected to oscillator circuit whereas other side of it has a connection to its bias voltage. The best selection under these considerations is Colpitts oscillator. Colpitts oscillator allows us to connect one side of the CMUT to the gate of its common-drain transistor while other side of the CMUT is connected to its bias voltage.

As we have discussed at the end of the chapter 2, the reactance of a CMUT is inductive between its parallel and series resonant frequencies, f_p and f_s, respectively. Again as it is shown in chapter 2, a CMUT has always a positive resistance due to radiation impedance on it. Therefore, a CMUT behaves like a lossy inductor between its parallel and series resonant frequencies. On the other hand, Colpitts oscillator acts like an active circuit and shows a negative resistance in addition to its capacitance. Therefore, by combining these two parts, we can obtain an CMUT based oscillator. This configuration can be represented as the following figure for the illustration purposes.

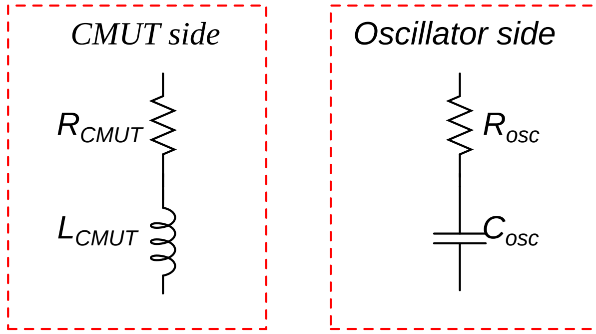

Figure 3.3: Illustration of CMUT between its series and parallel resonant frequencies and representation of Colpitts oscillator

In there, at a certain frequency (w_o) which is between the series and parallel resonant frequencies of the CMUT, we can achieve the conditions of

$$|R_{osc}| > R_{CMUT} \tag{3.7}$$

and

$$|\frac{1}{jw_oC_{osc}}| = |jw_oL_{CMUT}| \tag{3.8}$$

and have oscillation.

Chapter 4

CIRCUIT DESIGN

In this chapter, we will design a CMUT based Colpitts oscillator by depending on our previous discussions and investigate trade-offs associated with it.

4.1 CMUT based Colpitts Oscillator

As we have already explained at the end of chapter 3, we can obtain a CMUT based oscillator by connecting a CMUT with a Colpitts oscillator. This configuration can be portrayed as in Fig. 4.1.

In this circuitry, for Colpitts oscillator, it can be observed that we have a MOSFET as source follower and two capacitors. Therefore, the small signal equivalent circuit for Colpitts oscillator can be obtained as in Fig. 4.2.

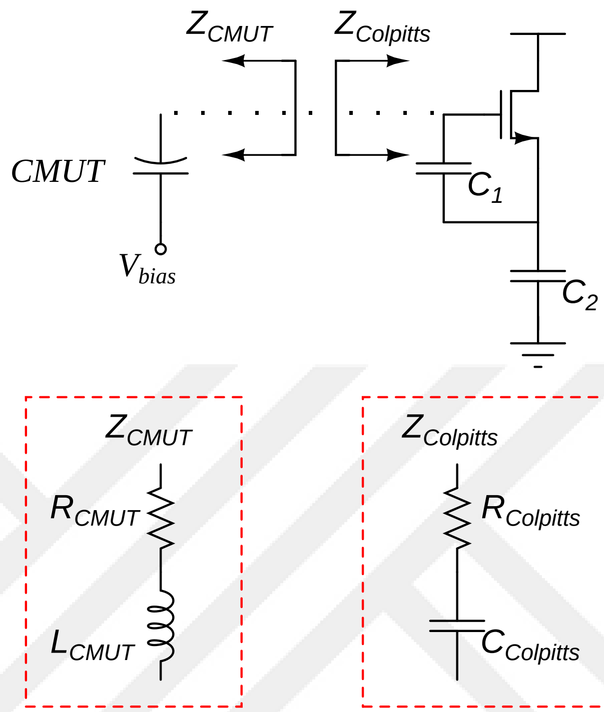

Figure 4.1: CMUT and Colpitts Oscillator

The impedance of this circuit ($Z_{Colpitts}$) which is seen by CMUT is

$$\begin{aligned} Z_{Colpitts} &= \frac{1}{jwC_1} + \frac{(jwC_1V_{gs} + g_mV_{gs})\frac{1}{jwC_2}}{jwC_1V_{gs}} \\ &= \frac{1}{jwC_1} - \frac{jwC_1 + g_m}{w^2C_1C_2} \\ &= -\frac{g_m}{w^2C_1C_2} + \frac{1}{jwC_1} + \frac{1}{jwC_2} \\ &= -\frac{g_m}{w^2C_1C_2} + \frac{1}{jwC_{HK}} \quad where \quad C_{HK} = \frac{C_1C_2}{C_1+C_2} \end{aligned} \tag{4.1}$$

As it can be seen from Eq. 4.1, real part of the impedance of the Colpitts oscillator is negative whereas imaginary part is capacitive. Thus, by combining Fig. 4.1 and Eq. 4.1, we can state that,

$$R_{Colpitts} = -\frac{g_m}{w^2C_1C_2} \tag{4.2}$$

and

$$C_{Colpitts} = \frac{C_1C_2}{C_1+C_2} \tag{4.3}$$

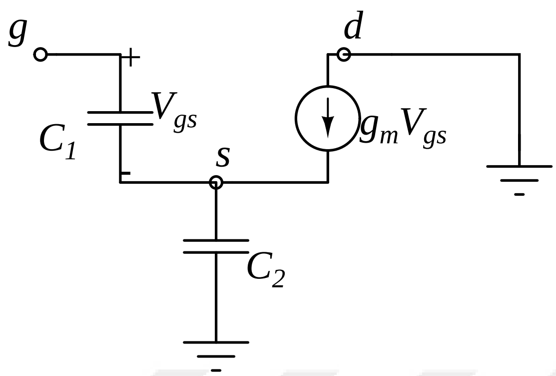

Figure 4.2: Small signal equivalent circuit for Colpitts oscillator

Now the questions are how are we going to choose C_1 and C_2 capacitance values, how our device can be more power efficient and what is the effect of C_1 and C_2 capacitance values on power efficiency.

Since we are designing a pressure sensor, we may want it to be portable and to work for long hours. In this respect, in order to achieve low power consumption, we have to minimize g_m of the transistor at the resonant frequency. As it can be observed in Eq. 4.2, on the other hand, negative resistance of the Colpitts oscillator depends on g_m and the product of C_1 and C_2. Therefore, in order to achieve minimum g_m, we have to minimize this product. In this respect, we have to select the right capacitance values and the right capacitance ratios that will help us to reduce the power consumption.

At the resonant frequency, we know that reactances of CMUT and Colpitts oscillator will be equal to each other. On the other hand, reactance of CMUT is determined by its geometrical and structural parameters and so it is fixed. Therefore, at resonant frequency $C_{Colpitts}$ will also be fixed. Under these consideration, assume that

$$C_2 = m \cdot C_1 \tag{4.4}$$

Then, from Eq. 4.3,

$$C_{Colpitts} = \frac{C_1 \cdot m \cdot C_1}{C_1 + m \cdot C_1} \tag{4.5}$$

and so

$$C_{Colpitts} = C_1 \cdot \frac{m}{m+1} \tag{4.6}$$

Therefore,

$$C_1 = C_{Colpitts} \cdot \frac{m+1}{m} \tag{4.7}$$

and

$$C_2 = C_{Colpitts} \cdot (m+1) \tag{4.8}$$

With these new C_1 and C_2, the product $C_1 \cdot C_2$ is

$$C_1 \cdot C_2 = C_{Colpitts}^2 \cdot \frac{(m+1)^2}{m} \tag{4.9}$$

In there, since $C_{Colpitts}$ is constant, in order to minimize the product we have to minimize $\frac{(m+1)^2}{m}$. Hence, from

$$\frac{d}{dm} \cdot \frac{(m+1)^2}{m} = 0 \tag{4.10}$$

we get

$$m = 1 \tag{4.11}$$

and so

$$C_1 = C_2 \tag{4.12}$$

Now, with Eq. 4.12, g_m in the Eq. 4.2 becomes

$$g_m = -R_{Colpitts} \cdot w^2 \cdot C_1 \cdot C_1 \tag{4.13}$$

In addition to that, for oscillation to occur, $|R_{Colpitts}| > R_{CMUT}$ must be achieved. Thus,

$$g_m > R_{CMUT} \cdot w^2 \cdot C_1 \cdot C_1 \tag{4.14}$$

Then, since

$$C_1 = C_2 = 2 \cdot C_{Colpitts} \tag{4.15}$$

g_m becomes

$$g_m > 4 \cdot R_{CMUT} \cdot w^2 \cdot C_{Colpitts}^2 \tag{4.16}$$

At this point, it is also possible to simplify the Eq. 4.16 more by benefiting the equation of

$$w \cdot C_{Colpitts} = \frac{1}{w \cdot L_{CMUT}} \tag{4.17}$$

Therefore, the Eq. 4.16 becomes

$$g_m > \frac{4 \cdot R_{CMUT}}{w^2 \cdot L_{CMUT}^2} \tag{4.18}$$

As it can be observed from the Eq. 4.18, there is a restriction on the minimum value of g_m. It is directly and inversely proportional with the real part (R_{CMUT}) and the square of the imaginary part ($w \cdot L_{CMUT}$) of the CMUT, respectively. Although Eq. 4.18 shows the restriction on the minimum value of g_m, it is arranged to be at least four times the minimum value required as the general rule of thumb to assure oscillation in the real life.

Up to this point, as it is indicated in chapter 3, we have analyzed our CMUT based Colpitts Oscillator design by depending on the negative resistance concept. However, again from chapter 3, we know that there is another method analyze oscillator circuits: feedback system approach. Therefore, now it is worth to analyze our CMUT based Colpitts Oscillator circuit with this analysis method and compare its results with what we have already obtained above.

4.2 Analysis of the Circuit based on Feedback System Approach

Consider the circuit given in the Fig. 4.1 again. As we already know, the gain of a source follower transistor is smaller than 1. Therefore, for oscillation to occur, ratio of the signal at the gate of this transistor to the signal at the source of the transistor must be greater than 1 so that total loop gain is greater than 1 (Barkhausen criteria). Another criterion is that the total phase of the loop have to be an integer multiple of 2π. The loop in the circuit can be represented as in Fig. 4.3. In this figure, we did not include the DC biasing parts in order not to deviate from the aim of this section and not to confuse the reader. The DC biasing circuits will be discussed in the next section.

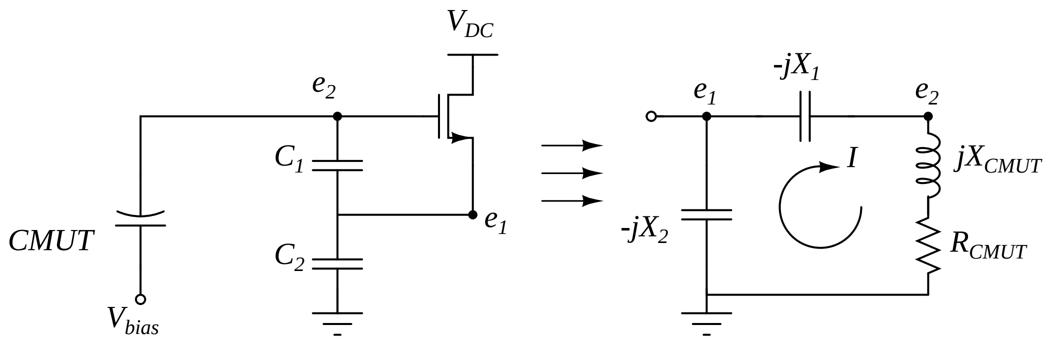

Figure 4.3: The loop in the CMUT based Colpitts oscillator circuit

In there,

$$X_1 = \frac{1}{w \cdot C_1} \tag{4.19}$$

$$X_2 = \frac{1}{w \cdot C_2} \tag{4.20}$$

and

$$X_{CMUT} = w \cdot L_{CMUT} \tag{4.21}$$

Therefore, by basing on this figure, we can say that

$$e_2 = I \cdot (R_{CMUT} + jX_{CMUT}) \tag{4.22}$$

and

$$e_1 = I \cdot (R_{CMUT} + jX_{CMUT} - jX_1) \tag{4.23}$$

Then, if we define A and β as

$$A = \frac{e_1}{e_2} \quad and \quad \beta = \frac{e_2}{e_1} \tag{4.24}$$

we can state that

$$\beta = \frac{e_2}{e_1} = \frac{I(R_{CMUT} + jX_{CMUT})}{I(R_{CMUT} + jX_{CMUT} - jX_1)} = \frac{R_{CMUT} + jX_{CMUT}}{R_{CMUT} + jX_{CMUT} - jX_1} \tag{4.25}$$

Since at the resonant frequency,

$$X_{CMUT} = X_1 + X_2 \tag{4.26}$$

Eq. 4.25 becomes

$$\beta = \frac{R_{CMUT} + jX_1 + jX_2}{R_{CMUT} + jX_1 + jX_2 - jX_1} = \frac{R_{CMUT} + jX_1 + jX_2}{R_{CMUT} + jX_2} \tag{4.27}$$

Then, because the value of R_{CMUT} is generally small compared to X_1 and X_2, Eq. 4.27 simplifies to

$$\beta = \frac{X_1 + X_2}{X_2} \tag{4.28}$$

At this point, from Barkhausen criteria we can derive that

$$A \cdot \beta \geq 1 \tag{4.29}$$

and

$$\angle A\beta = 2n\pi \quad where \quad n = 0, 1, 2, ... \tag{4.30}$$

Then, since the small signal gain for a source follower (common-drain) MOSFET is

$$A = \frac{g_m Z_L}{1 + g_m Z_L} \tag{4.31}$$

we have to check whether

$$\left(\frac{g_m Z_L}{1 + g_m Z_L}\right) \cdot \left(\frac{X_1 + X_2}{X_2}\right) \geq 1 \tag{4.32}$$

and

$$\angle\left(\frac{g_m Z_L}{1 + g_m Z_L}\right)\left(\frac{X_1 + X_2}{X_2}\right) = 2n\pi \quad where \quad n = 0, 1, 2, ... \tag{4.33}$$

Now, look at the e_1 point in Fig. 4.3. Z_L shows the seen impedance from this point. Therefore,

$$Z_L = \frac{-jX_2 \cdot (R_{CMUT} + jX_{CMUT} - jX_1)}{R_{CMUT} + jX_{CMUT} - jX_1 - jX_2} \tag{4.34}$$

Then, since at the resonant frequency $X_{CMUT} = X_1 + X_2$, Z_L becomes

$$\begin{aligned} Z_L &= \frac{-jX_2 \cdot (R_{CMUT} + jX_1 + jX_2 - jX_1)}{R_{CMUT} + jX_1 + jX_2 - jX_1 - jX_2} \\ &= \frac{-jX_2 \cdot (R_{CMUT} + jX_2)}{R_{CMUT}} \\ &= \frac{-jX_2 \cdot R_{CMUT} + X_2^2}{R_{CMUT}} \\ &= \frac{X_2 \cdot (-jR_{CMUT} + X_2)}{R_{CMUT}} \end{aligned} \tag{4.35}$$

Then, as it is stated before, since the value of R_{CMUT} is generally small compared to X_2, Eq. 4.35 simplifies to

$$Z_L = \frac{X_2^2}{R_{CMUT}} \tag{4.36}$$

At that point, by depending on Eq. 4.33 and Eq. 4.36, it can be declared that at the frequency of oscillation we have no phase shift. Since we have satisfied that the phase condition of the Barkhausen criteria, next we have to check the gain criterion. For this purpose, if we put Z_L from Eq. 4.36 into Eq. 4.32, we get

$$\left(\frac{g_m\left(\frac{X_2^2}{R_{CMUT}}\right)}{1+g_m\left(\frac{X_2^2}{R_{CMUT}}\right)}\right)\cdot\left(\frac{X_1+X_2}{X_2}\right)\geq 1 \tag{4.37}$$

and

$$\left(\frac{g_m X_2^2}{R_{CMUT}+g_m X_2^2}\right)\cdot\left(\frac{X_1+X_2}{X_2}\right)\geq 1 \tag{4.38}$$

and

$$g_m\cdot X_2\cdot(X_1+X_2)\geq R_{CMUT}+g_m\cdot X_2^2 \tag{4.39}$$

and so

$$g_m\cdot X_1\cdot X_2+g_m\cdot X_2^2\geq R_{CMUT}+g_m\cdot X_2^2 \tag{4.40}$$

and finally

$$g_m\cdot X_1\cdot X_2\geq R_{CMUT} \tag{4.41}$$

It can be easily observed that Eq. 4.18 and Eq. 4.41 are exactly the same results. For Eq. 4.41, if we assume $C_1 = C_2$, $C_1 = C_2 = 2\cdot C_{Colpitts}$ and $w\cdot C_{Colpitts} = \frac{1}{w\cdot L_{CMUT}}$, we obtain the same equations.

Therefore, it can be concluded that our CMUT based Colpitts oscillator circuit works according to the both analysis methods (negative resistance concept and feedback system approach) under some certain conditions, as it is expected.

4.3 DC Biasing of the Colpitts Oscillator

DC biasing is very important in our design. We want our dc biasing circuit not to cause loading effect on the loop. In our circuit there exist two DC biasing circuits. One of them biases the source follower (common-drain) transistor at its source and other one biases the CMUT and gate of the source follower transistor.

The bias circuit at the source of the amplifier will be parallel to $C2$ capacitor of the Colpitts oscillator. Therefore, by depending on the resistance, it will cause loading on the resonator. To avoid it, we need to keep bias resistance seen by the Colpitts oscillator as high as possible.

There are two possible ways of achieving biasing: using a resistor directly and benefiting from a current mirror circuit. Among these methods, however, utilizing a current mirror circuit is more logical because of the main two disadvantages of using a resistor directly.
1) A high valued resistor will have a high voltage difference on it. Thus, it will limit the oscillator swing.
2) Since we are designing an integrated circuit, we want our components to take a small space. A high valued resistance, however, will take a lot of place compared to a transistor.

Similarly, the bias circuit at the gate of the amplifier will cause loading on the resonator by depending on the resistance. Therefore, we can again benefit from current mirror circuits and construct a stabilized bias circuit with transistors.

Under these considerations, we can design the bias circuit with the Colpitts oscillator as in Fig. 4.4.

In there, PMOS transistors (M_4, M_5) and NMOS transistors (M_2, M_3) are for the stabilized bias circuit to bias the CMUT and the gate of the amplifier. NMOS transistor (M_1), on the other hand, is for the current mirror circuit to bias the source of the amplifier. In addition to that, the process name is C35B4C3, transistor library is PRIMLIB and cellnames are pmosm4 for PMOS transistors and nmosm4 for NMOS transistors. Beside these, breakdown voltage for the transistors is 5.5 V.

As for the capacitors C_1 and C_2, by depending on the Eqs. 4.2, 4.18 and 4.41, it can be deduced that it is better to choose their values as small as possible.

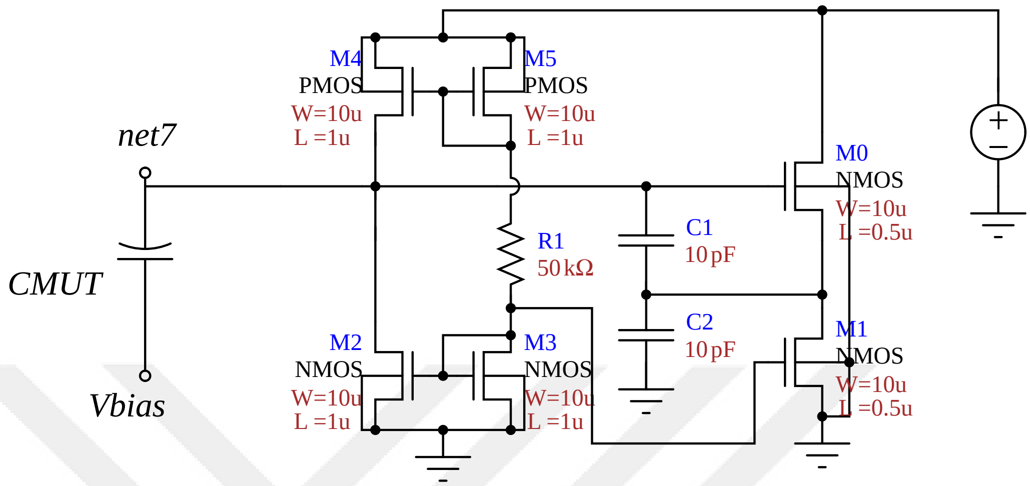

Figure 4.4: DC bias circuit with the Colpitts oscillator

However, in reality we will confront with some extra capacitances like stray parasitic capacitance and pad capacitance. Therefore, it is generally recommended not to select them too low. With this consideration, we have decided to use 10 pF capacitors for C_1 and C_2.

We have selected V_{DC} as the standard 5 V and; hence, we have obtained an oscillating signal approximately between 5 V and 0 V at the gate of the transistor M_0 i.e. net7 as in Fig. 4.5. Beside all of these, V_{bias} has been obtained from the charge pump circuit as 15 V.

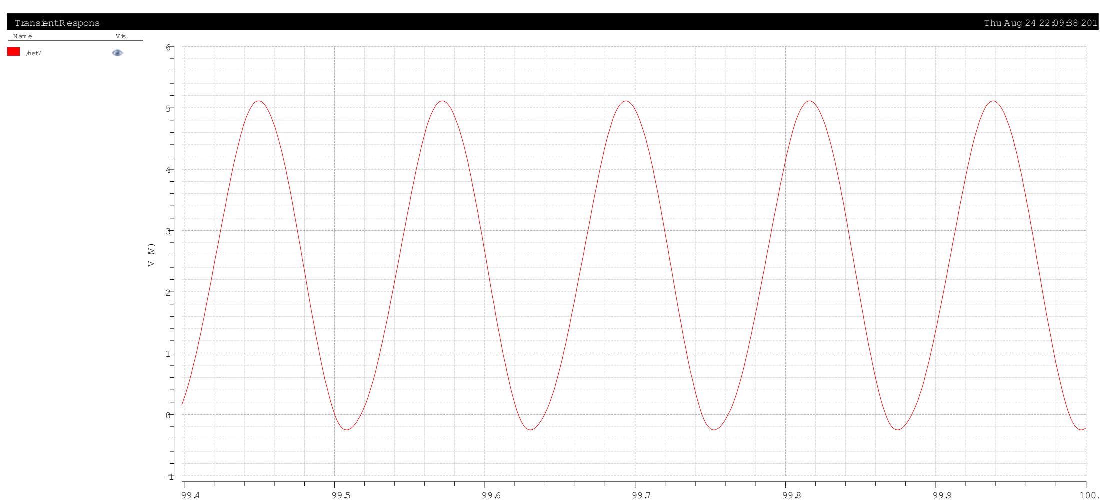

Figure 4.5: Oscillating signal approximately between 5 V and 0 V

4.4 Ring Oscillator

In order to obtain V_{bias} voltage on the CMUT, we have decided to utilize a charge pump circuit. In this respect, first of all, we have designed a ring oscillator circuit to obtain oscillating signals for the charge pump circuit.

In the ring oscillators, in order not to cause latchup, the total number of inverters in the loop must be odd. If the circuit latches up, it stucks in a state and remains in there indefinitely instead of making oscillation. In addition to that, due to inverter delay, adding too many inverters to the loop enhances the total period of oscillation and so frequency of oscillation decreases. We want high frequency oscillating signals in our charge pump circuit in order to use low value capacitors as possible and to charge up these capacitors as fast as possible. Therefore, so as to obtain highest possible frequency of oscillation, we have used a three stage ring oscillator as in Fig. 4.6.

In this design, the transistor sizes are arranged to obtain the oscillating signals between 5V and 0V as possible. In addition to that, again in there, the process name is C35B4C3, transistor library is PRIMLIB and cellnames are pmosm4 for PMOS transistors and nmosm4 for NMOS transistors. Beside these, breakdown voltage for the transistors is 5.5 V.

When we obtain oscillations from this circuit, we have 180 degree phase shift between the gates of the transistor M_6 and M_7, and drains of the transistor M_{10} and M_{11} due to Barkhausen criteria. Therefore, there exists 60 degree phase shift between each consecutive stage in addition to a signal inversion. With this respect, the oscillating signal at each net can be observed as in Fig. 4.7. The oscillation frequency of the circuit is 1.7 GHz.

4.5 Charge Pump Circuit

Since from the ring oscillator circuit we have 3 nets that carry distinct oscillating signals, in order to benefit all of them, we have decided to design a voltage quadrupler circuit. Therefore, we have designed the circuit in Fig. 4.8.

In there, net4, net5 and net6 are same with the Fig. 4.7. Therefore, with this configuration, signals charge up capacitors C_3, C_4, C_5 and C_6 by passing through the diodes D_0, D_1, D_2 and D_3. However, the turn-on voltages of the diodes are 0.7 V and the oscillating signals do not oscillate exactly between 5 V and zero due to resistors of diodes in the small signal equivalent circuit. In addition to that, due to capacitances on the diodes, oscillation frequencies on the net4, net5 and net6 a little bit slow down and becomes 150 MHz. With this respect, in order to make ripple voltage on V_{bias} net minimum enough, we have chosen the values of the capacitors C_3, C_4, C_5 and C_6 as 50 pF.

As mentioned above, there are 60 degree phase difference between net4, net5 and net6 and it causes 0.9 V loss on C_4 and C_5 during their charging. Therefore, after taking all these losses into account, we have obtained V_{bias} as 4·5 - 4·0.7 - 2·0.9 - 0.4 (due to not having oscillating signals exactly between 5 V and 0 V) = 15 V. The simulation results for the charge pump circuit and voltages on each net can be observed in Fig. 4.9.

4.6 Final Design

The final design for the CMUT based Colpitts oscillator and its layout in CADENCE can be observed in Fig. 4.10 and Fig. 4.11, respectively. The total area of the layout is 730 μm $\cdot$ 840 μm = 0.6132 mm^2.

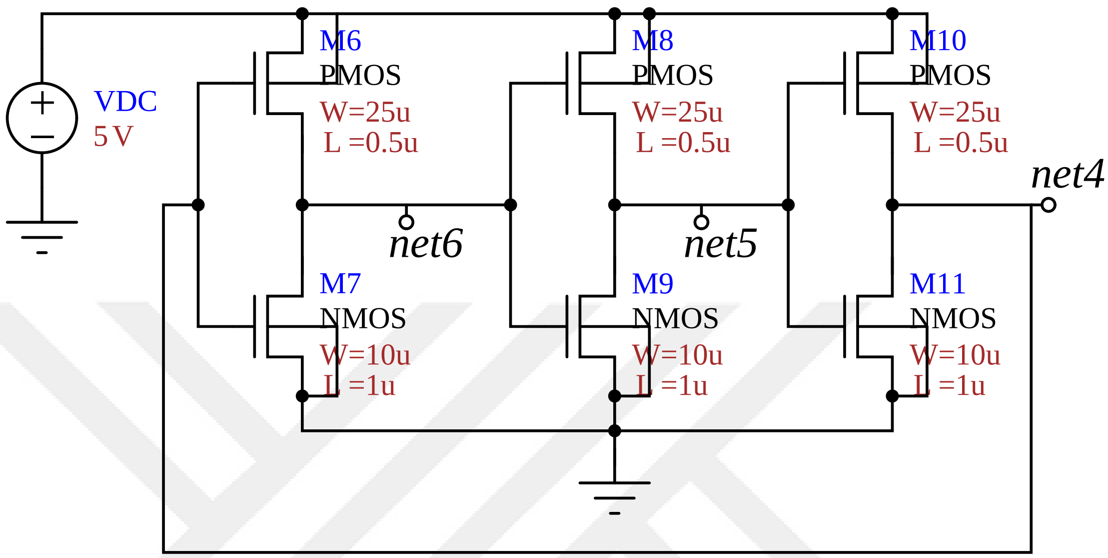

Figure 4.6: Design for the three stage ring oscillator [6]

Figure 4.7: Oscillating signal at each stage of the three stage ring oscillator

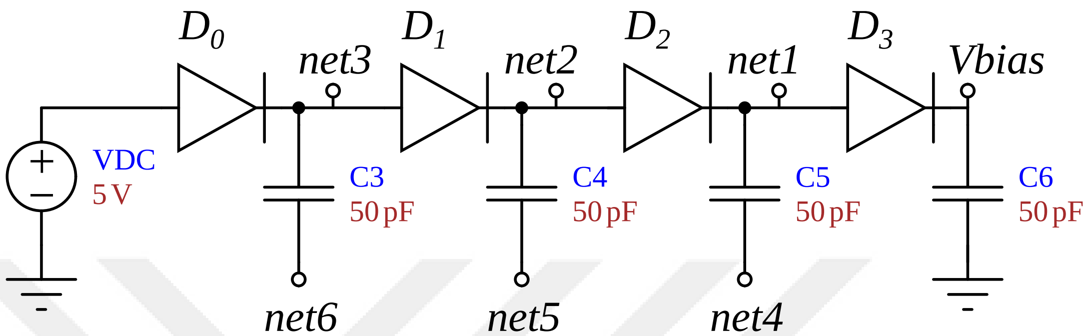

Figure 4.8: Voltage quadrupler circuit [7]

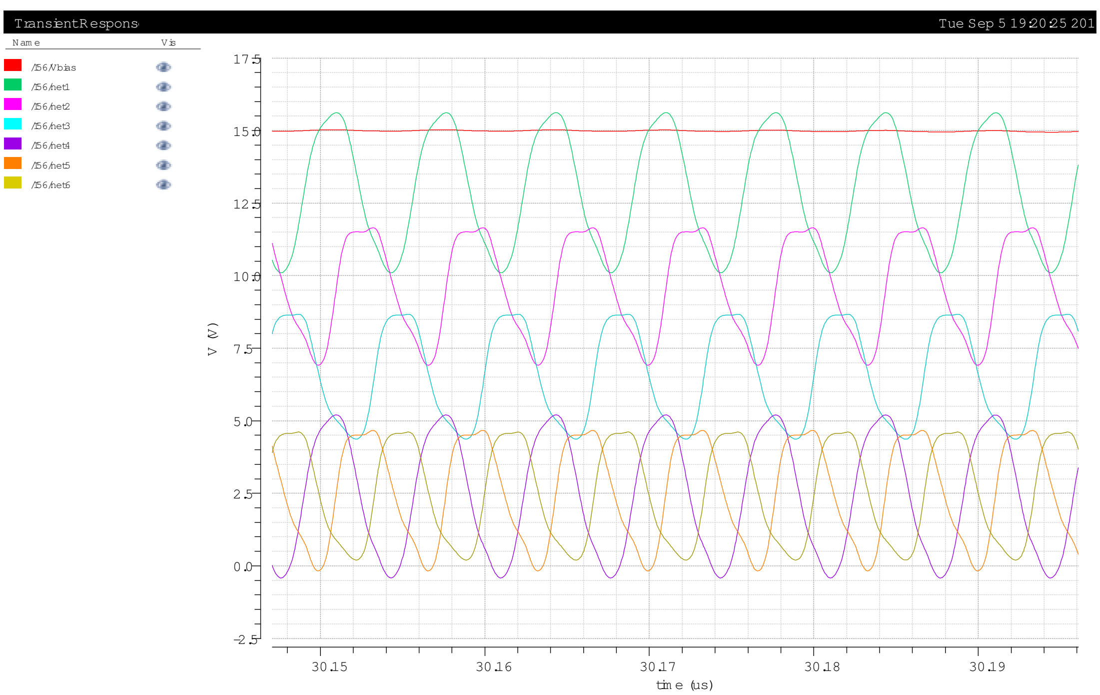

Figure 4.9: Simulation results for the charge pump circuit and voltages on each net

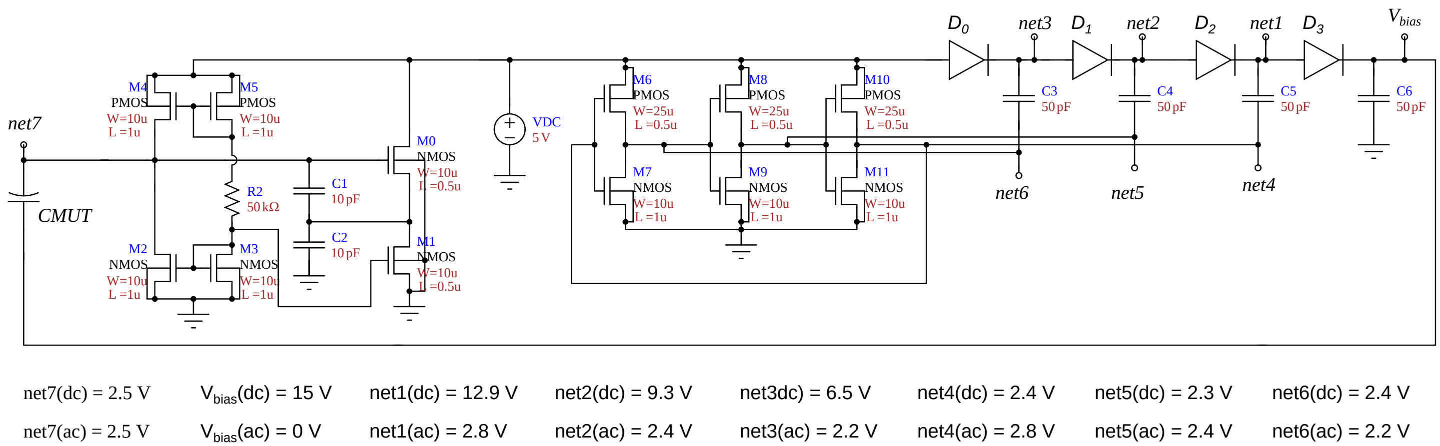

Figure 4.10: Final design for the CMUT based Colpitts oscillator

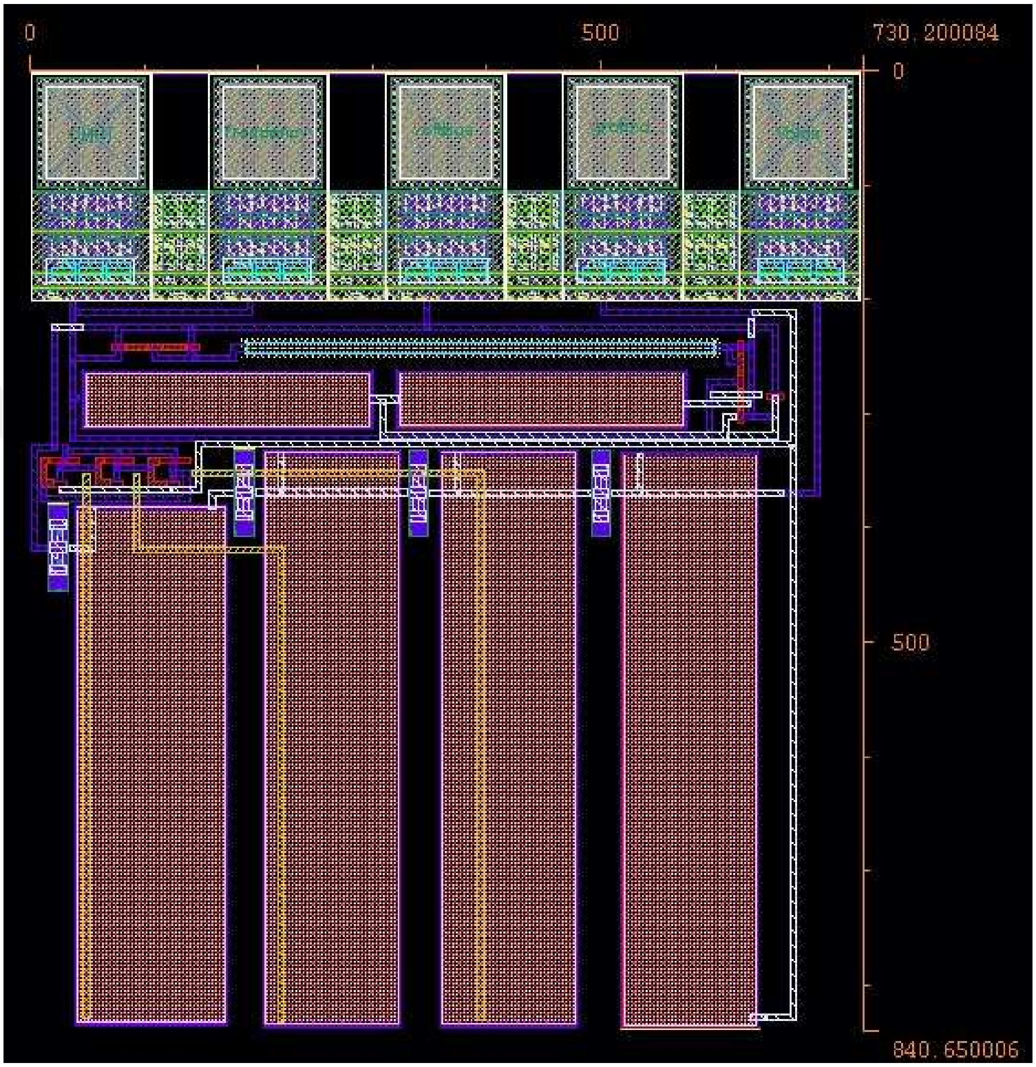

Figure 4.11: Layout of the CMUT based Colpitts oscillator

The diode parameters are 3.0534e-10 m^2 for "device area" and 880.8 μm for "perimeter". The breakdown voltages for the diodes are 9 V. Layout of the diodes are same with the diodes in the pads. However, since the substrate is a p-type substrate, diodes are put into a n-well in the layout. Two dimensional view representation of the diodes is as in Fig. 4.12.

Two dimensional view representations of a NMOS transistor, a PMOS transistor and the resistor, on the other hand, are as in Fig. 4.13, Fig. 4.14 and Fig. 4.15, respectively.

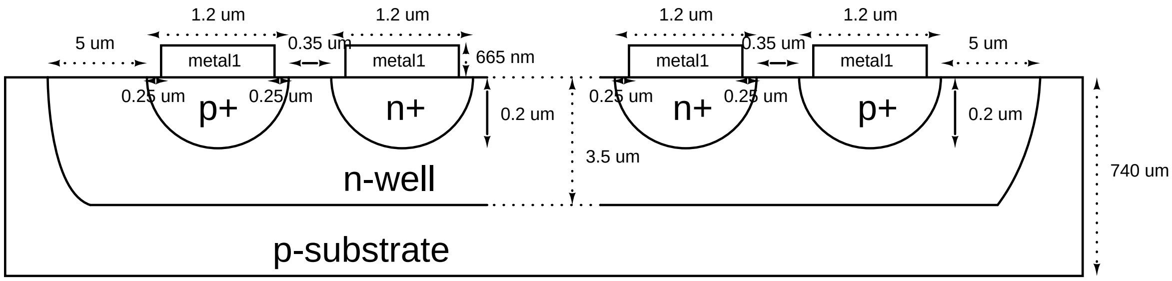

Figure 4.12: Two dimensional view representation of the diodes

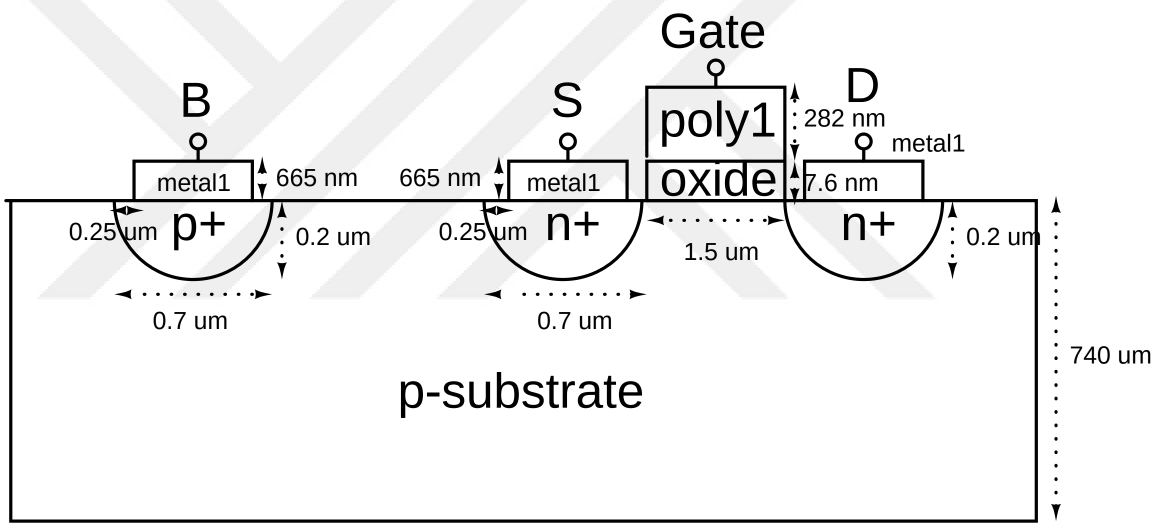

Figure 4.13: Two dimensional view representation of a NMOS transistor

With this section, we have concluded our CMUT based Colpitts oscillator circuit design. Now, in the next chapter we will discuss how we have constructed the optimum CMUT.

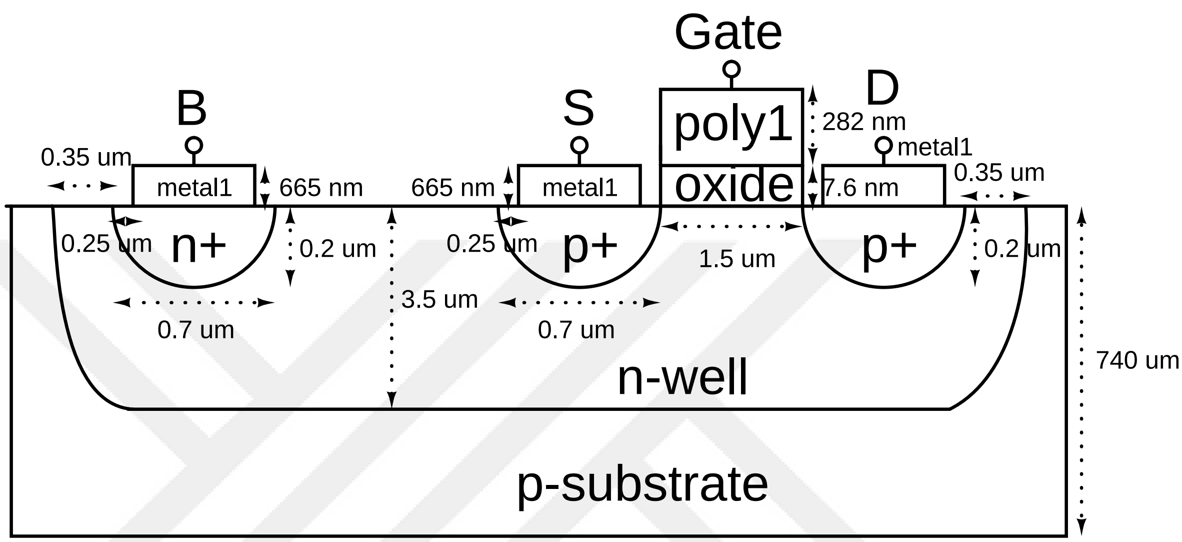

Figure 4.14: Two dimensional view representation of a PMOS transistor

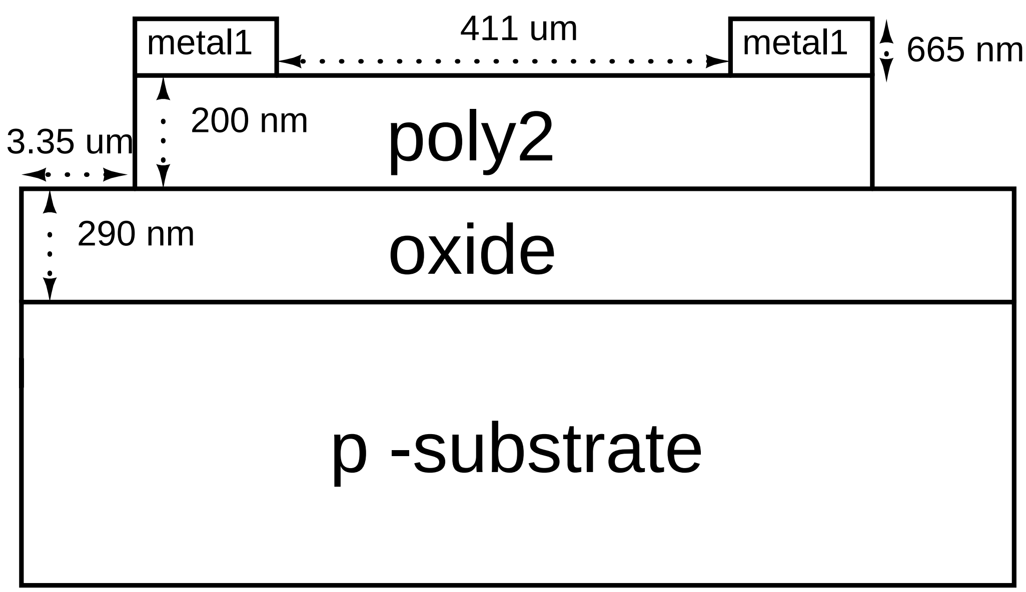

Figure 4.15: Two dimensional view representation of the resistor

Chapter 5

OPTIMUM CMUT

In order to obtain the optimum CMUT, first of all, we will calculate the *sensitivity*. All of the MATLAB codes related to this chapter can be found in Appendix A. The MATLAB version we have used is R2013a.

5.1 Calculation of Sensitivity

In Section 2.2, we have obtained simplified CMUT small signal equivalent circuit and calculated its equivalent impedance (Z_{CMUT}). In addition to that in Section 4.1, we have shown how to represent Colpitts oscillator with parameters of $R_{Colpitts}$ and $C_{Colpitts}$. In this respect, by assuming that we meet the requirement indicated by Eq. 3.7,

$$|R_{Colpitts}| > R_{CMUT} \tag{5.1}$$

where

$$R_{CMUT} = \mathbb{R}\text{e}\{Z_{CMUT}\} \tag{5.2}$$

At resonant frequency we have

$$|\frac{1}{jw_o C_{Colpitts}}| = |jw_o L_{CMUT}| \tag{5.3}$$

where

$$L_{CMUT} = \mathbb{Im}\{Z_{CMUT}\} \tag{5.4}$$

Thus, the resonant frequency (f_0) is

$$f_0 = \frac{1}{2\pi\sqrt{L_{CMUT}C_{Colpitts}}} \tag{5.5}$$

From Eq. 2.20 we can deduce R_{CMUT} and L_{CMUT}. Since

$$R_{CMUT} + jw_oL_{CMUT} = Z_{CMUT} \tag{5.6}$$

and so

$$R_{CMUT} + jw_oL_{CMUT} = \frac{\left(R_{eq} + jw_oL_{eq} + \frac{1}{jw_oC_{eq}}\right)\left(\frac{1}{jw_oC_{0d}}\right)}{\left(R_{eq} + jw_oL_{eq} + \frac{1}{jw_o}\left(\frac{1}{C_{eq}} + \frac{1}{C_{0d}}\right)\right)} \tag{5.7}$$

we can find L_{CMUT} as

$$L_{CMUT} = \frac{-w_o^4L_{eq}^2C_{eq}^2C_{0d} + 2w_o^2L_{eq}C_{eq}C_{0d} + w_o^2L_{eq}C_{eq}^2 - w_o^2R_{eq}^2C_{eq}^2C_{0d} - C_{0d} - C_{eq}}{(-w_o^2R_{eq}C_{eq}C_{0d})^2 + (-w_o^3L_{eq}C_{eq}C_{0d} + w_oC_{0d} + w_oC_{eq})^2} \tag{5.8}$$

and R_{CMUT} as

$$R_{CMUT} = \frac{w_o^2R_{eq}C_{eq}^2}{(-w_o^2R_{eq}C_{eq}C_{0d})^2 + (-w_o^3L_{eq}C_{eq}C_{0d} + w_oC_{0d} + w_oC_{eq})^2} \tag{5.9}$$

As it can be seen, L_{CMUT} already depends on f_o; hence, finding f_o from Eq. 5.5 is very tedious. In this respect, we need a simpler equation for resonant frequency.

In section 2.2, we have shown how to find series and parallel resonant frequencies of a CMUT. Hence, under the condition of Eq. 5.1, since $C_{Colpitts}$ will actually be parallel to C_{0d}, we can write the resonant frequency (f_o) as

$$f_0 = \frac{1}{2\pi\sqrt{L_{eq}\left(\frac{C_{eq}(C_{0d}+C_{Colpitts})}{C_{eq}+C_{0d}+C_{Colpitts}}\right)}} \tag{5.10}$$

Therefore, f_o is

$$f_0 = \frac{1}{2\pi\sqrt{\frac{1}{n_R^2}\left(L_{Rm} + \mathbb{Im}\{Z_{RR}\}\right)\left(\frac{n_R^2\left(\frac{(-C_{RS})(C_{Rm})}{(-C_{RS})+(C_{Rm})}\right)\left(C_0g\left(\frac{X_P}{tge}\right)+C_{Colpitts}\right)}{n_R^2\left(\frac{(-C_{RS})(C_{Rm})}{(-C_{RS})+(C_{Rm})}\right)+C_0g\left(\frac{X_P}{tge}\right)+C_{Colpitts}}\right)}} \tag{5.11}$$

Now, since $\mathbb{Im}\{Z_{RR}\}$ is negligible compared to L_{Rm} and since C_{RS} is considerably larger than C_{Rm}, we can simplify this equation as

$$f_0 = \frac{1}{2\pi\sqrt{\frac{L_{Rm}}{n_R^2}\frac{n_R^2 C_{Rm}\left(C_0 g\left(\frac{X_P}{t_{ge}}\right)+C_{Colpitts}\right)}{n_R^2 C_{Rm}+C_0 g\left(\frac{X_P}{t_{ge}}\right)+C_{Colpitts}}}} \tag{5.12}$$

Then, if we put the values of each parameter, we get

$$f_0 = \frac{1}{2\pi\sqrt{\frac{\frac{9}{5}\rho\pi\frac{(1-\sigma^2)}{16\pi Y_0}\frac{a^4}{t_m^2}\left(\epsilon_0\frac{\pi a^2}{t_{ge}}g\left(\frac{X_P}{t_{ge}}\right)+C_{Colpitts}\right)}{\frac{9\pi\epsilon_0^2 V_{DC}^2(1-\sigma^2)}{16Y_0}\left(g'\left(\frac{X_P}{t_{ge}}\right)\right)^2\frac{a^6}{t_{ge}^4 t_m^3}+\epsilon_0\frac{\pi a^2}{t_{ge}}g\left(\frac{X_P}{t_{ge}}\right)+C_{Colpitts}}}} \tag{5.13}$$

At this point, since the values of $g\left(\frac{X_P}{t_{ge}}\right)$ and $g'\left(\frac{X_P}{t_{ge}}\right)$ does not change so much, for simplification purposes, we can define some constants such as

$$A = \frac{9}{5}\rho\pi\frac{(1-\sigma^2)}{16\pi Y_0} \tag{5.14}$$

$$B = \epsilon_0\pi g\left(\frac{X_P}{t_{ge}}\right) \tag{5.15}$$

and

$$C = \frac{9\pi\epsilon_0^2 V_{DC}^2(1-\sigma^2)}{16Y_0}\left(g'\left(\frac{X_P}{t_{ge}}\right)\right)^2 \tag{5.16}$$

and simplify the f_0 equation further as

$$f_0 = \frac{1}{2\pi\sqrt{\frac{A\frac{a^4}{t_m^2}\left(B\frac{a^2}{t_{ge}}+C_{Colpitts}\right)}{C\frac{a^6}{t_{ge}^4 t_m^3}+B\frac{a^2}{t_{ge}}+C_{Colpitts}}}} \tag{5.17}$$

and so

$$f_0 = \frac{1}{2\pi}\sqrt{\frac{C\frac{a^6}{t_{ge}^4 t_m^3}+B\frac{a^2}{t_{ge}}+C_{Colpitts}}{A\frac{a^4}{t_m^2}\left(B\frac{a^2}{t_{ge}}+C_{Colpitts}\right)}} \tag{5.18}$$

As it can be seen in the latest equation of f_0, it only depends on the geometrical parameters of CMUT: a, t_m and t_{ge}.

In references [1] and [2], we have an equation related the forces on a CMUT as

$$\frac{F_{Pb}}{F_{Pg}} = \frac{\frac{1}{3}\pi a^2 P_0}{\frac{t_{ge}}{5C_{Rm}}} = \frac{3\pi a^4 P_0(1-\sigma^2)}{16\pi Y_0 t_{ge} t_m^3} \tag{5.19}$$

where F_{Pb} is the external static force and F_{Pg} is the force required to make the deflection of the top plate at its center equal to the effective gap height. If we assume Eq. 5.19 equals to a constant, we get

$$P_0 = \frac{16\pi(\frac{F_{Pb}}{F_{Pg}})Y_0 t_{ge} t_m^3}{3\pi a^4(1-\sigma^2)} \tag{5.20}$$

Therefore, under a certain pressure, we get a constant K_1 as

$$K_1 = \frac{a^4}{t_{ge} t_m^3} \tag{5.21}$$

In addition to that, we obtain $\frac{V_c}{V_r}$ the ratio of the collapse voltage (V_c) to V_r from the references [1] and [2]

$$\frac{V_c}{V_r} \approx 0.9961 - 1.0468\frac{F_{Pb}}{F_{Pg}} + 0.06972\Big(\frac{F_{Pb}}{F_{Pg}} - 0.25\Big)^2 + 0.01148\Big(\frac{F_{Pb}}{F_{Pg}}\Big)^6 \tag{5.22}$$

also as a constant. Since V_{DC} is constant, if we take $\frac{V_{DC}}{V_c}$ equal to a constant such as 0.8, V_c and so V_r becomes constant. Therefore, from Eq. 2.6, we can write V_r as

$$V_r = 8\frac{t_{ge}}{\sqrt{K_1}}\sqrt{\frac{Y_0}{27\epsilon_0(1-\sigma^2)}} \tag{5.23}$$

and obtain t_{ge} as

$$t_{ge} = \frac{V_r\sqrt{K_1}}{8}\sqrt{\frac{27\epsilon_0(1-\sigma^2)}{Y_0}} \tag{5.24}$$

We can get $\frac{df_0}{dt_m}$ as

$$\begin{aligned}\frac{df_0}{dt_m} = {} & \frac{1}{4\pi}\left(\frac{-3C\frac{a^6}{t_{ge}^4 t_m^4}}{(A\frac{a^4}{t_m^2}(B\frac{a^2}{t_{ge}} + C_{Colpitts}))^{1/2}(C\frac{a^6}{t_{ge}^4 t_m^3} + B\frac{a^2}{t_{ge}} + C_{Colpitts})^{1/2}}\right) \\ & - \frac{1}{4\pi}\left(\frac{(-2A\frac{a^4}{t_m^3}(B\frac{a^2}{t_{ge}} + C_{Colpitts}))(C\frac{a^6}{t_{ge}^4 t_m^3} + B\frac{a^2}{t_{ge}} + C_{Colpitts})^{1/2}}{(A\frac{a^4}{t_m^2}(B\frac{a^2}{t_{ge}} + C_{Colpitts}))^{3/2}}\right)\end{aligned} \tag{5.25}$$

Hence, with these new equations and under these above assumptions, we can rewrite $\frac{df_0}{dt_m}$ as

$$\frac{df_0}{dt_m} = \frac{1}{4\pi}\left(\frac{-3Ct_m^{\frac{1}{2}}K_1^{\frac{3}{2}}t_{ge}^{\frac{-5}{2}}}{(At_mK_1t_{ge}(Bt_m^{\frac{3}{2}}K_1^{\frac{1}{2}}t_{ge}^{\frac{-1}{2}}+C_{Colpitts}))^{1/2}(Ct_m^{\frac{3}{2}}K_1^{\frac{3}{2}}t_{ge}^{\frac{-5}{2}}+Bt_m^{\frac{3}{2}}K_1^{\frac{1}{2}}t_{ge}^{\frac{-1}{2}}+C_{Colpitts})^{1/2}}\right) - \frac{1}{4\pi}\left(\frac{(-2AK_1t_{ge}(Bt_m^{\frac{3}{2}}K_1^{\frac{1}{2}}t_{ge}^{\frac{-1}{2}}+C_{Colpitts}))(Ct_m^{\frac{3}{2}}K_1^{\frac{3}{2}}t_{ge}^{\frac{-5}{2}}+Bt_m^{\frac{3}{2}}K_1^{\frac{1}{2}}t_{ge}^{\frac{-1}{2}}+C_{Colpitts})^{1/2}}{(At_mK_1t_{ge}(Bt_m^{\frac{3}{2}}K_1^{\frac{1}{2}}t_{ge}^{\frac{-1}{2}}+C_{Colpitts}))^{3/2}}\right) \tag{5.26}$$

Beside that, from Eq. 5.20, we can obtain $\frac{dP_0}{dt_m}$ as

$$\frac{dP_0}{dt_m} = \frac{16(\frac{F_{Pb}}{F_{Pg}})Y_0t_{ge}t_m^2}{a^4(1-\sigma^2)} = \frac{16(\frac{F_{Pb}}{F_{Pg}})Y_0}{(1-\sigma^2)K_1t_m} \tag{5.27}$$

Finally, $\frac{df_0}{dP_0}$ is

$$\frac{df_0}{dt_m} = \frac{K_1t_m(1-\sigma^2)}{64\pi(\frac{F_{Pb}}{F_{Pg}})Y_0}\left(\frac{-3Ct_m^{\frac{1}{2}}K_1^{\frac{3}{2}}t_{ge}^{\frac{-5}{2}}}{(At_mK_1t_{ge}(Bt_m^{\frac{3}{2}}K_1^{\frac{1}{2}}t_{ge}^{\frac{-1}{2}}+C_{Colpitts}))^{1/2}(Ct_m^{\frac{3}{2}}K_1^{\frac{3}{2}}t_{ge}^{\frac{-5}{2}}+Bt_m^{\frac{3}{2}}K_1^{\frac{1}{2}}t_{ge}^{\frac{-1}{2}}+C_{Colpitts})^{1/2}}\right) - \frac{K_1t_m(1-\sigma^2)}{64\pi(\frac{F_{Pb}}{F_{Pg}})Y_0}\left(\frac{(-2AK_1t_{ge}(Bt_m^{\frac{3}{2}}K_1^{\frac{1}{2}}t_{ge}^{\frac{-1}{2}}+C_{Colpitts}))(Ct_m^{\frac{3}{2}}K_1^{\frac{3}{2}}t_{ge}^{\frac{-5}{2}}+Bt_m^{\frac{3}{2}}K_1^{\frac{1}{2}}t_{ge}^{\frac{-1}{2}}+C_{Colpitts})^{1/2}}{(At_mK_1t_{ge}(Bt_m^{\frac{3}{2}}K_1^{\frac{1}{2}}t_{ge}^{\frac{-1}{2}}+C_{Colpitts}))^{3/2}}\right) \tag{5.28}$$

Therefore, $\frac{df_0}{dP_0}$ versus $\frac{F_{Pb}}{F_{Pg}}$ for different values of t_m at $P_0 = 1$ atm can be observed as in Fig. 5.1.

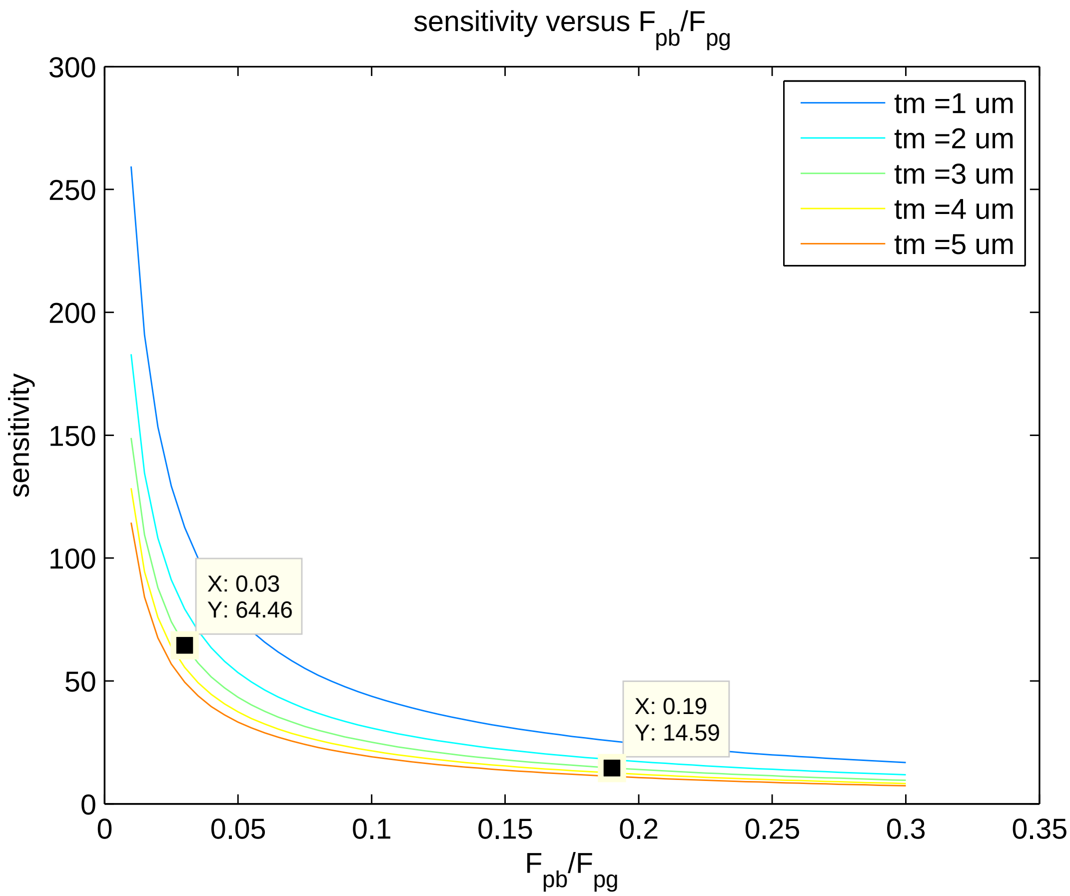

Figure 5.1: $\frac{df_0}{dP_0}$ versus $\frac{F_{Pb}}{F_{Pg}}$ for different values of t_m

5.2 Calculation of the Quality Factor

In order to reduce the phase noise, we need a circuit that has high Quality factor. Therefore, it is reasonable to calculate the Quality factor of our circuit.

As we said before, in our circuit, capacitors C_1 and C_2 are equal to each other and at resonant frequency CMUT behaves like a lossy inductor. In addition to that due to dc biasing circuit, we have bias resistances on the circuit. In this respect, if we call the output resistance due to transistors M_4 and M_5 as R1, the output resistance due to transistors M_2 and M_3 as R2 and the output resistance due to transistor M_1 as R3, in small signal we obtain the circuit in Fig. 5.2.

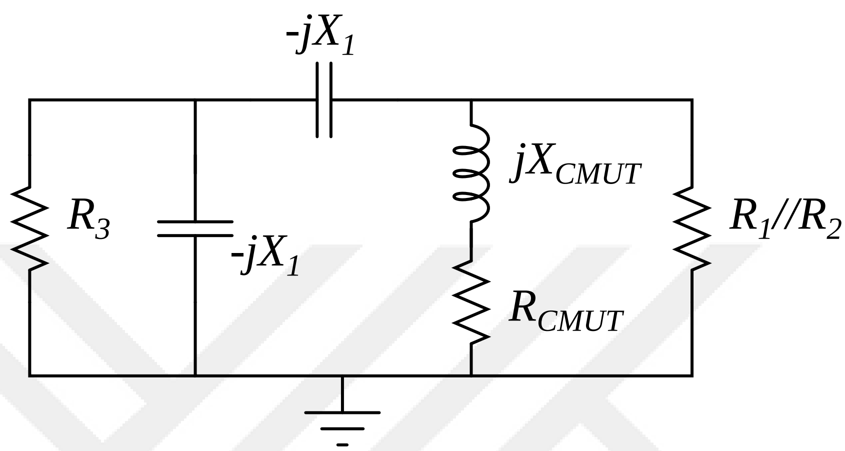

Figure 5.2: Overall CMUT based Colpitts oscillator in small signal

In this configuration, first of all, we have to make a series RL to parallel RL circuit transition for R_{CMUT} and L_{CMUT}. If we say parallel resistance is R_p and series inductance is L_p, their values becomes

$$R_p = \frac{w_0^2 L_{CMUT}^2 + R_{CMUT}^2}{R_{CMUT}} \tag{5.29}$$

and

$$L_p = \frac{w_0^2 L_{CMUT}^2 + R_{CMUT}^2}{w_0^2 L_{CMUT}} \tag{5.30}$$

Beside that we have to convert R_3 and both $-jX_1$s into a parallel RC circuit. Hence, if we say R_{p2} and C_p for the resistance and the capacitance, respectively for this new circuit, we obtain their values as

$$R_{p2} = \frac{1 + 4w_0^2 C_1^2 R_3^2}{w_0^2 C_1^2 R_3} \tag{5.31}$$

and

$$C_p = \frac{C_1 + 2w_0^2 C_1^3 R_3^2}{1 + 4w_0^2 C_1^2 R_3^2} \tag{5.32}$$

Therefore, our new circuit with these new parameters is

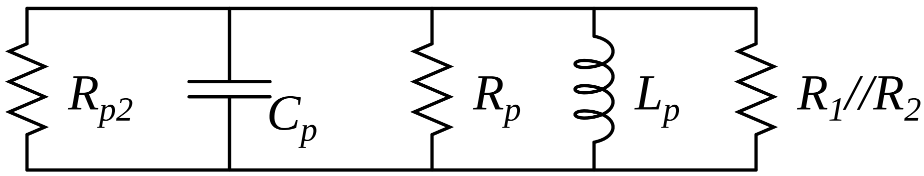

Figure 5.3: Overall CMUT based Colpitts oscillator in small signal with new parameters

and hence the Quality factor for this parallel RLC circuit is

$$Q = \frac{(R_{p2}//R_p//R_1//R_2)}{w_0 L_p} = w_0 C_p (R_{p2}//R_p//R_1//R_2) \tag{5.33}$$

5.3 Temperature (T) Sensitivity

The effect of the temperature on the CMUT have been patented [34]. According to it, the temperature induced deflection (h) is

$$h = \frac{M}{2 \cdot D}\ a_{TE}^2 \log(\frac{a}{a_{TE}}) \tag{5.34}$$

where a_{TE}, M and D are the radius of the top electrode from the center point of the cavity, the thermally induced momentum of the top plate and the flexural rigidity of the plate, respectively. In addition to that

$$D = \frac{Y_0 \cdot t_m^3}{12 \cdot (1 - \sigma^2)} \tag{5.35}$$

and

$$M = S \cdot \big((t_i + t_{TE} - \frac{t_m}{2})^2 - (t_i - \frac{t_m}{2})^2\big) \tag{5.36}$$

where t_{TE} is the thickness of the top electrode and S is the radial thermal stress [18, 35]:

$$S = \frac{Y_0 \cdot \alpha \cdot \Delta T}{(1 - \sigma)} \tag{5.37}$$

where ΔT is the temperature difference between top plate and substrate and α is the thermal expansion coefficient. For a PECVD SiN_x, α has the value of $3.27 \cdot 10^{-6}\ ^{\circ}C^{-1}$ [36].

As we know from the references [1, 2, 21], our CMUT model in chapter 2 agrees well with the real CMUT profiles when $a_i/a \leq 0.25$ and $a_0/a \geq 0.8$. In addition to that as it can be deduced from Section 5.1, *sensitivity* increases as the thickness of the insulator layer (t_i) decreases. Therefore, since we want a thin insulator layer, we may not have M equal to zero by arranging the thickness of the insulator layer (t_i). In this case, best way of producing a temperature insensitive CMUT is doing $a = a_{TE}$ and so providing the top electrode to cover all the top plate area.

5.4 Selection of the Optimum CMUT

While selecting the optimum CMUT, we will assume that we are using Silicon Nitride (Si_3N_4) in our top plate and; therefore, we will take CMUT parameters of relative permittivity of the insulator (ϵ_r), Young's modulus of the top plate (Y_0), Poisson's ratio of the top plate (σ) and density of the top plate (ρ) as 5.4, 115 GPa, 0.27 and 3100 kg/m^3, respectively as they are indicated in references [1] and [21]. In addition to that since we are designing a pressure sensor which will function in an aerial environment, we will take speed of sound in the immersion medium (c) as 340 m/s and density of the immersion medium (ρ_0) as

$$\rho_0 = \frac{P_0}{R \cdot T} \tag{5.38}$$

where R is the ideal gas constant (287.058 (J/(kg·K)) [37]) and T is temperature in Kelvin (K). At $P_0 = 1$ atm and T $= 15°C$, the value of ρ_0 becomes 1.225 kg/m^3 [38].

We want our device to function in the pressure interval of 0-1 atm with the highest possible frequency versus pressure *sensitivity*. On the other hand, due to restrictions in the production process, our CMUT needs to be feasible in the clean rooms. In this respect, the gap height of the cell (t_g) should not be too low such as 5-10 nm, the thickness of the top plate (t_m) should not be too high like 9-10 μm and due to dielectric breakdown field (E_{brk}) value of Silicon Nitride (Si_3N_4), the thickness of the insulator layer (t_i) should not be less than

$\frac{15\ V}{E_{brk}} = \frac{15\ V}{1000\ V/\mu m} = 15$ nm [21, 39]. In addition to that, although in theory 15 nm is enough, so as to keep a safety margin the thickness of the insulator layer (t_i) should be chosen at least two times larger. The following figure shows t_{ge} values against $\frac{F_{Pb}}{F_{Pg}}$ for different values of t_m at $P_0 = 1$ atm.

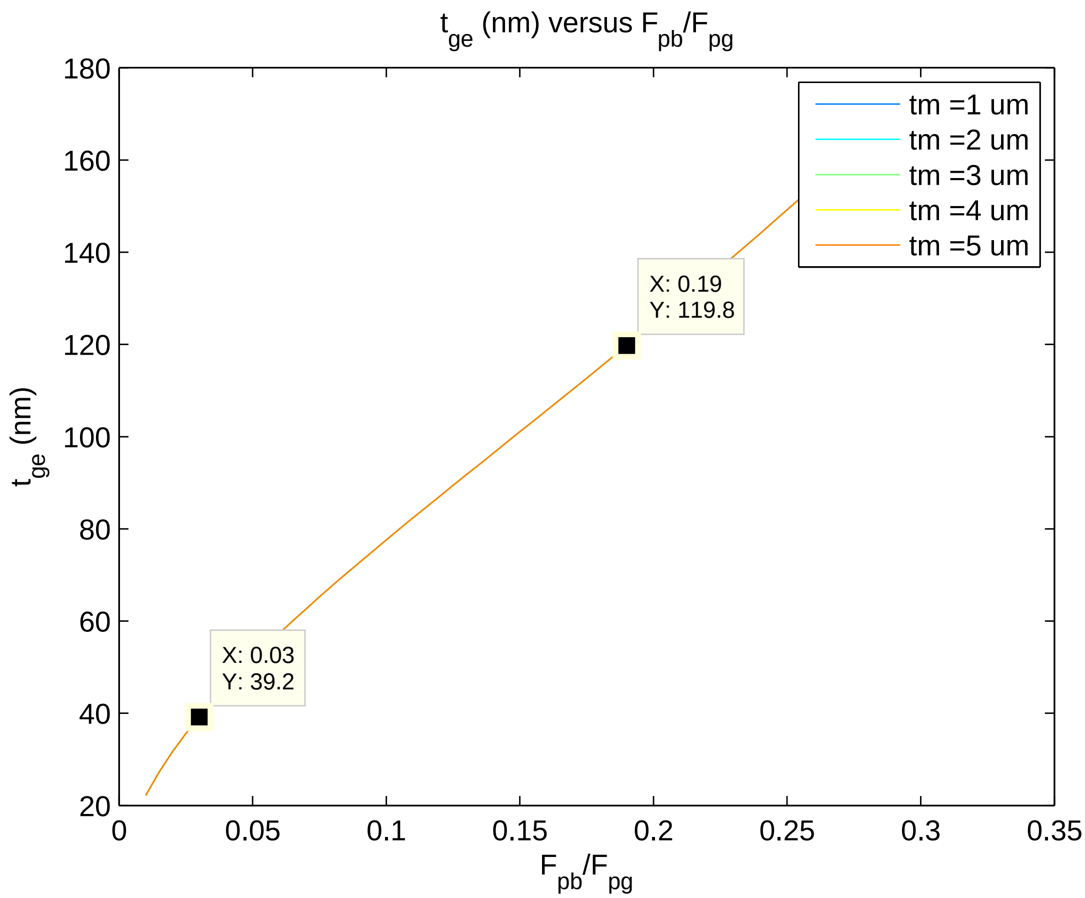

Figure 5.4: t_{ge} versus $\frac{F_{Pb}}{F_{Pg}}$ for different values of t_m

Beside these, in order to obtain oscillations R_{CMUT} should be maximum around 1500 ohm. Fig. 5.5 shows R_{CMUT} versus $\frac{F_{Pb}}{F_{Pg}}$ for different values of t_m at $P_0 =$ 1 atm.

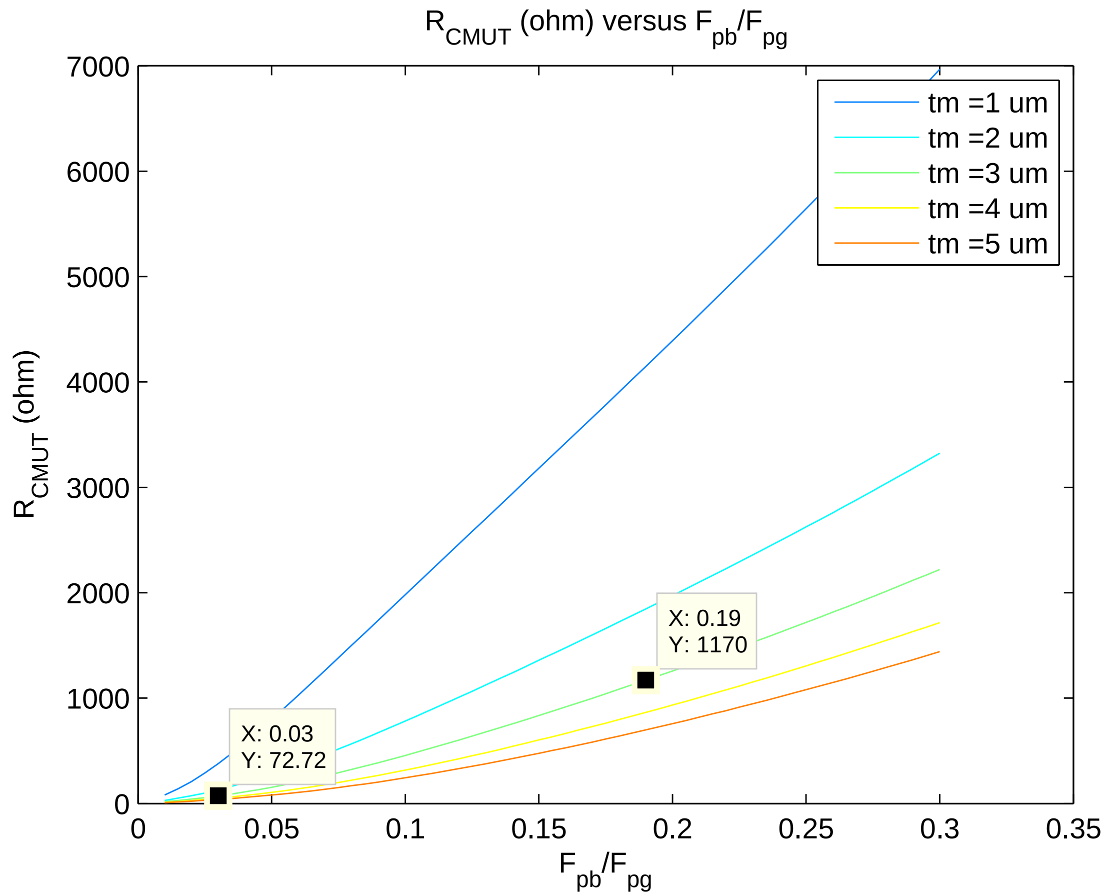

Figure 5.5: R_{CMUT} versus $\frac{F_{Pb}}{F_{Pg}}$ for different values of t_m

Under the consideration of all above discussions; therefore, we have decided the optimum CMUT parameters as

Optimum CMUT Parameters		
a	44 μm	21 μm
t_g	100 nm	34 nm
t_i	100 nm	30 nm
t_m	3 μm	3 μm
V_{DC}	12.5 V	12.5 V
V_c	15.9 V	16.4 V
sensitivity	14.6 Hz/Pa	64.5 Hz/Pa
ϵ_r (Si_3N_4)	5.4	5.4
Y_0 (Si_3N_4)	115 GPa	115 GPa
σ (Si_3N_4)	0.27	0.27
ρ (Si_3N_4)	3100 kg/m^3	3100 kg/m^3

Table 5.1: Optimum parameters for the CMUT

In there, although the sensitivity of the second design is better, due to practicability of CMUT in the clean room, we have decided to select the first design. Then, at $P_0 = 1$ atm, the resonant frequency is 3.9 MHz and the sensitivity is 14.6 Hz/Pa. In addition to that, since R_1 is 360K, R_2 is 360K and R_3 is 70K, the Quality factor of the circuit is 5 and the inherent Quality factor of the CMUT is 432.

With this circuit configuration even at maximum atmospheric pressure 107 kPa, deflection of the top plate at its center (X_P) becomes 40.4 nm. Therefore, our CMUT does not collapse and works in the uncollapsed mode as intended. Beside that, a system is considered as elastically linear if X_P levels up to 20% of the thickness of the top plate (t_m) [40, 41]. Hence, since in our circuit $\frac{X_P}{t_m} = \frac{40.4\ nm}{3\ \mu m} = 0.0135$, it is elastically linear.

Chapter 6

CONCLUSION

In this thesis, we have designed a CMUT based Colpitts oscillator which works as a pressure sensor which measures pressure between zero atm and one atm with *sensitivity* of 14.6 Hz/Pa at 1 atm.

We have started the design of our device from CMUT. Therefore, first of all, we have examined the small signal equivalent circuit model and the related analytical equations that helps to model the behavior of an uncollapsed mode CMUT from [1, 2, 3, 23]. Then, we have taken or derived necessary equations from them for our study and coded in the MATLAB. Also, we have simplified the equations to liken the CMUT to a crystal oscillator.

Secondly, we have investigated oscillators. Thus, firstly, we have discussed the analytical methods which help us to understand whether an oscillator circuit works or not. The analytical methods we have investigated are the "feedback system approach" and the "negative resistance concept". Then, by being based on the some certain criteria we have decided to use a Colpitts oscillator.

Thirdly, we have designed the oscillator circuit for our CMUT based Colpitts oscillator design; and then, by depending on the analytical methods we have discussed, we have derived the restrictions on the circuit parameters for a power efficient device. In addition to that, we have mentioned how to bias the oscillator without causing any loading effect on the oscillator circuit. Then, we have designed a ring oscillator and a charge pump circuit and have obtained the V_{bias} voltage for the CMUT. We have also given the final design for our circuit.

Finally, we have calculated the *sensitivity* of a CMUT and the Quality factor of our circuit. Then, we have mentioned the calculation of the temperature sensitivity of a CMUT and by being based on these calculations, we have selected the optimum CMUT.

Bibliography

[1] H. K. Oğuz, *Circuit theory based modeling and analysis of CMUT arrays.* PhD thesis, Bilkent University, 2013.

[2] H. Koymen, A. Atalar, E. Aydogdu, C. Kocabas, H. K. Oguz, S. Olcum, A. Ozgurluk, and A. Unlugedik, "An improved lumped element nonlinear circuit model for a circular CMUT cell," *IEEE Transactions on Ultrasonics, Ferroelectrics and Frequency Control*, vol. 59, no. 8, 2012.

[3] "Bilkent University CMUT Research Group." http://cmut.bilkent.edu.tr/.

[4] H. Jaffe and P. SMITH, "IRE standards on piezoelectric crystals-the piezoelectric vibrator-definitions and methods of measurement, 1957," *Proceedings of the Institute of Radio Engineers*, vol. 45, no. 3, pp. 353–358, 1957.

[5] D. M. Pozar, *Microwave Engineering.* John Wiley & Sons, 2005.

[6] B. Razavi, *Design of Analog CMOS Integrated Circuits.* McGraw-Hill, 2001.

[7] G. Di Cataldo and G. Palumbo, "Dynamic analysis of 3 stage dickson voltage multiplier for an optimized design," in *Electrotechnical Conference, 1994. Proceedings., 7th Mediterranean*, pp. 633–636, IEEE, 1994.

[8] D. Zhao, S. Zhuang, and R. Daigle, "A commercialized high frequency CMUT probe for medical ultrasound imaging," in *Ultrasonics Symposium (IUS), 2015 IEEE International*, pp. 1–4, IEEE, 2015.

[9] Verasonics, "L22-8v CMUT Linear Array." http://verasonics.com/l22-8v-cmut-linear-array/.

[10] J. D. Fraser, “Bias charge regulator for capacitive micromachined ultrasonic transducers,” Dec. 11 2001. US Patent 6,328,696.

[11] H. Wang, X. Wang, C. He, and C. Xue, “Design and performance analysis of capacitive micromachined ultrasonic transducer linear array,” *Micromachines*, vol. 5, no. 3, pp. 420–431, 2014.

[12] H. Lee, K. Park, P. Cristman, O. Oralkan, M. Kupnik, and B. Khuri-Yakub, “A low-noise oscillator based on a multi-membrane CMUT for high sensitivity resonant chemical sensors,” in *Micro Electro Mechanical Systems, 2009. MEMS 2009. IEEE 22nd International Conference on*, pp. 761–764, IEEE, 2009.

[13] M. Kumar, C. Seok, M. Mahmud, X. Zhang, and O. Oralkan, “A low-power integrated circuit for interfacing a capacitive micromachined ultrasonic transducer (CMUT) based resonant gas sensor,” in *Sensors, 2015 IEEE*, pp. 1–4, IEEE, 2015.

[14] H. J. Lee, K. K. Park, O. Oralkan, M. Kupnik, and B. T. Khuri-Yakub, “CMUT as a chemical sensor for DMMP detection,” in *Frequency Control Symposium, 2008 IEEE International*, pp. 434–439, IEEE, 2008.

[15] H. J. Lee, K. K. Park, P. Cristman, O. Oralkan, M. Kupnik, and B. T. Khuri-Yakub, “The effect of parallelism of CMUT cells on phase noise for chem/bio sensor applications,” in *Ultrasonics Symposium, 2008. IUS 2008. IEEE*, pp. 1951–1954, IEEE, 2008.

[16] H. J. Lee, K. K. Park, Ö. Oralkan, M. Kupnik, and B. T. Khuri-Yakub, “A multichannel oscillator for a resonant chemical sensor system,” *IEEE Transactions on Industrial Electronics*, vol. 61, no. 10, pp. 5632–5640, 2014.

[17] F. Mohit Kumar *et al.*, “A low-power integrated interface circuit for a resonant gas sensor based on a capacitive micromachined ultrasonic transducer (CMUT),” 2015.

[18] Z. Li, L. Zhao, Z. Jiang, S. Akhbari, J. Ding, Y. Zhao, Y. Zhao, and L. Lin, “Capacitive micromachined ultrasonic transducer for ultra-low pressure measurement: Theoretical study,” *AIP Advances*, vol. 5, no. 12, p. 127231, 2015.

[19] Z. Li, L. Zhao, Z. Jiang, Z. Ye, and Y. Zhao, "Capacitive micromachined ultrasonic transducer for ultra-low pressure detection," in *Nano/Micro Engineered and Molecular Systems (NEMS), 2014 9th IEEE International Conference on*, pp. 600–603, IEEE, 2014.

[20] Z. Li, L. Zhao, Z. Ye, H. Wang, Y. Zhao, and Z. Jiang, "Resonant frequency analysis on an electrostatically actuated microplate under uniform hydrostatic pressure," *Journal of Physics D: Applied Physics*, vol. 46, no. 19, p. 195108, 2013.

[21] S. Olçum, *Deep collapse mode capacitive micromachined ultrasonic transducers.* PhD thesis, Bilkent University, 2010.

[22] S. Olcum, F. Y. Yamaner, A. Bozkurt, and A. Atalar, "Deep-collapse operation of capacitive micromachined ultrasonic transducers," *IEEE Transactions on Ultrasonics, Ferroelectrics and Frequency Control*, vol. 58, no. 11, 2011.

[23] H. K. Oguz, A. Atalar, and H. Köymen, "Equivalent circuit-based analysis of CMUT cell dynamics in arrays," *IEEE Transactions on Ultrasonics, Ferroelectrics and Frequency Control*, vol. 60, no. 5, pp. 1016–1024, 2013.

[24] E. Aydoğdu, *Lumped element modeling of circular CMUT in collapsed mode.* PhD thesis, Bilkent University, 2014.

[25] E. Aydogdu, A. Ozgurluk, A. Atalar, and H. Koymen, "Lumped element modeling of CMUT arrays in collapsed mode," in *Ultrasonics Symposium (IUS), 2014 IEEE International*, pp. 309–312, IEEE, 2014.

[26] D. Southworth, H. Craighead, and J. Parpia, "Pressure dependent resonant frequency of micromechanical drumhead resonators," *Applied Physics Letters*, vol. 94, no. 21, p. 213506, 2009.

[27] Q. Stedman, K. K. Park, and B. T. Khuri-Yakub, "CMUT chip with integrated temperature and pressure sensors," in *Ultrasonics Symposium (IUS), 2016 IEEE International*, pp. 1–4, IEEE, 2016.

[28] M. A. Fonseca, J. M. English, M. Von Arx, and M. G. Allen, "Wireless micromachined ceramic pressure sensor for high-temperature applications," *Journal of Microelectromechanical Systems*, vol. 11, no. 4, pp. 337–343, 2002.

[29] I. Ladabaum, X. Jin, H. T. Soh, A. Atalar, and B. Khuri-Yakub, "Surface micromachined capacitive ultrasonic transducers," *IEEE Transactions on Ultrasonics, Ferroelectrics and Frequency Control*, vol. 45, no. 3, pp. 678–690, 1998.

[30] H. K. Oguz, S. Olcum, M. N. Senlik, V. Tas, A. Atalar, and H. Koymen, "Nonlinear modeling of an immersed transmitting capacitive micromachined ultrasonic transducer for harmonic balance analysis," *IEEE Transactions on Ultrasonics, Ferroelectrics and Frequency Control*, vol. 57, no. 2, 2010.

[31] M. N. Senlik, S. Olcum, H. Koymen, and A. Atalar, "Radiation impedance of an array of circular capacitive micromachined ultrasonic transducers," *IEEE Transactions on Ultrasonics, Ferroelectrics and Frequency Control*, vol. 57, no. 4, 2010.

[32] M. N. Şenlik, *Radiation impedance of capacitive micromachined ultrasonic transducers*. PhD thesis, Bilkent University, 2010.

[33] N. M. Nguyen and R. G. Meyer, "Start-up and frequency stability in high-frequency oscillators," *IEEE Journal of Solid-State Circuits*, vol. 27, no. 5, pp. 810–820, 1992.

[34] P. Dirksen and A. Leeuwestein, "Temperature compensation in a CMUT device," Jan. 24 2017. US Patent 9,550,211.

[35] S. Talebian, G. Rezazadeh, M. Fathalilou, and B. Toosi, "Effect of temperature on pull-in voltage and natural frequency of an electrostatically actuated microplate," *Mechatronics*, vol. 20, no. 6, pp. 666–673, 2010.

[36] C.-L. Tien and T.-W. Lin, "Thermal expansion coefficient and thermomechanical properties of SiNx thin films prepared by plasma-enhanced chemical vapor deposition," *Applied Optics*, vol. 51, no. 30, pp. 7229–7235, 2012.

[37] T. Foken, *Micrometeorology.* Springer, 2017.

[38] M. Ragheb, "Air Density at Standard Temperature and Pressure." http://mragheb.com/NPRE%20475%20Wind%20Power%20Systems/.

[39] C. Ng, K. Chew, and S. Chu, "Characterization and comparison of PECVD silicon nitride and silicon oxynitride dielectric for MIM capacitors," *IEEE Electron Device Letters*, vol. 24, no. 8, pp. 506–508, 2003.

[40] A. Unlugedik, A. S. Tasdelen, A. Atalar, and H. Koymen, "Designing transmitting CMUT cells for airborne applications," *IEEE Transactions on Ultrasonics, Ferroelectrics, and Frequency Control*, vol. 61, no. 11, pp. 1899–1910, 2014.

[41] E. Ventsel and T. Krauthammer, *Thin plates and shells: theory: analysis, and applications.* CRC press, 2001.

Appendix A

CMUT MATLAB Code

A.1 CMUT.m

```
% CMUT SMALL SIGNAL MODEL

%PARAMETERS
%++++++++++++++++++++++++++++++++++++++++++++++++++++++++++++++++
%The parameters below have been taken from work of Huseyin Kagan
%Oguz: "http://repository.bilkent.edu.tr/handle/11693/15881"
%and formulas have been taken from: "http://cmut.bilkent.edu.tr/?page_id=6"
er = 5.4; %relative permittivity of the insulator
%Po = 101325; %ambient pressure %standard sea level atmospheric pressure is
    101325 pascals (https://en.wikipedia.org/wiki/Pressure)
Yo = 115*10^9; %(115 GPa) Young's modulus of the top plate
sigma = 0.27; %Poisson's ratio of the top plate
ro = 3100; %(3100 kg/m^3) density of the top plate
%++++++++++++++++++++++++++++++++++++++++++++++++++++++++++++++++

%DEFINITION OF FOUND PARAMETERS INSIDE THE FORMULAS
%++++++++++++++++++++++++++++++++++++++++++++++++++++++++++++++++
%tge is the effective gap height
%Vr is the collapse voltage in the absence of ambient pressure
%CRm represents the compliance of the top plate
%LRm is due to mass of the top plate
%XP is the deflection of the top plate at its center
%nR is the turns ratio of electromechanical transformer
%C0d is the input electrical capacitance including the effect of top plate
    deflection
%CRS arises from the spring-softening effect
%++++++++++++++++++++++++++++++++++++++++++++++++++++++++++++++++
```

```
%EXTRA PARAMETERS
%++++++++++++++++++++++++++++++++++++++++++++++++++++++++++++
eo = 8.854187817*10^-12; %(https://en.wikipedia.org/wiki/Vacuum_permittivity)
                          %1/(36*pi*10^9) %permittivity of free space
%++++++++++++++++++++++++++++++++++++++++++++++++++++++++++++

% FpbOverFpg = 0.01:0.01:0.99;
FpbOverFpg = 0.01:0.01:0.05;
tm = 1*10^-6:1*10^-6:5*10^-6; %thickness of the top plate

VcOverVr = zeros(size(tm,2),size(FpbOverFpg,2));
Vr = zeros(size(tm,2),size(FpbOverFpg,2));
K1 = zeros(size(tm,2),size(FpbOverFpg,2));
tge = zeros(size(tm,2),size(FpbOverFpg,2));
a = zeros(size(tm,2),size(FpbOverFpg,2));
CRm = zeros(size(tm,2),size(FpbOverFpg,2));
eqn = zeros(size(tm,2),size(FpbOverFpg,2));
XP_values = zeros(size(tm,2),size(FpbOverFpg,2));
XP = zeros(size(tm,2),size(FpbOverFpg,2));
B = zeros(size(tm,2),size(FpbOverFpg,2));
C = zeros(size(tm,2),size(FpbOverFpg,2));
sensitivity = zeros(size(tm,2),size(FpbOverFpg,2));
mult = zeros(size(tm,2),size(FpbOverFpg,2));
num1 = zeros(size(tm,2),size(FpbOverFpg,2));
den1 = zeros(size(tm,2),size(FpbOverFpg,2));
num2 = zeros(size(tm,2),size(FpbOverFpg,2));
den2 = zeros(size(tm,2),size(FpbOverFpg,2));
Co = zeros(size(tm,2),size(FpbOverFpg,2));
LRm = zeros(size(tm,2),size(FpbOverFpg,2));
nR = zeros(size(tm,2),size(FpbOverFpg,2));
C0d = zeros(size(tm,2),size(FpbOverFpg,2));
CRS = zeros(size(tm,2),size(FpbOverFpg,2));
K = zeros(size(tm,2),size(FpbOverFpg,2));
Ceq = zeros(size(tm,2),size(FpbOverFpg,2));
Leq = zeros(size(tm,2),size(FpbOverFpg,2));
fp = zeros(size(tm,2),size(FpbOverFpg,2));
fs = zeros(size(tm,2),size(FpbOverFpg,2));
fo = zeros(size(tm,2),size(FpbOverFpg,2));
wavenumber = zeros(size(tm,2),size(FpbOverFpg,2));
ka = zeros(size(tm,2),size(FpbOverFpg,2));
radiationImpedance = zeros(size(tm,2),size(FpbOverFpg,2));
Req = zeros(size(tm,2),size(FpbOverFpg,2));
Qcmut = zeros(size(tm,2),size(FpbOverFpg,2));
Zcmut = zeros(size(tm,2),size(FpbOverFpg,2));
Rcmut = zeros(size(tm,2),size(FpbOverFpg,2));
Lcmut = zeros(size(tm,2),size(FpbOverFpg,2));
Rp = zeros(size(tm,2),size(FpbOverFpg,2));
Lp = zeros(size(tm,2),size(FpbOverFpg,2));
Rp2 = zeros(size(tm,2),size(FpbOverFpg,2));
```

```
Cp = zeros(size(tm,2),size(FpbOverFpg,2));
Rparallel = zeros(size(tm,2),size(FpbOverFpg,2));
Qcircuit = zeros(size(tm,2),size(FpbOverFpg,2));

for kk = 1:size(tm,2)
    kk
    VcOverVr(kk,:) = 0.9961 - 1.0468.*FpbOverFpg + 0.06972.*(FpbOverFpg-0.25).^2
         + 0.01148*(FpbOverFpg).^6;
    Vdc = 12.5;
    VdcOverVc = 0.8;
    Vc = Vdc/VdcOverVc;
    Vr(kk,:) = Vc./VcOverVr(kk,:);

    atm = 1;
    atmToPascal = 101325; %ambient pressure %standard sea level atmospheric
        pressure is 101325 pascals (https://en.wikipedia.org/wiki/Pressure)
    Po = atm*atmToPascal;

    % K1 = a^4/(tge*tm^3);
    K1(kk,:)= (FpbOverFpg*16*pi*Yo)/(3*pi*Po*(1-sigma^2));

    % Vr = 8* (((tm^1.5) * (tge^1.5))/(a^2))* sqrt(Yo/(27*eo*(1-sigma^2)));
    % Vr = 8* (tge/sqrt(K1))* sqrt(Yo/(27*eo*(1-sigma^2)));
    tge(kk,:) = (Vr(kk,:).*sqrt(K1(kk,:))/8).*sqrt((27*eo*(1-sigma^2))/(Yo));

    a(kk,:) = (K1(kk,:).*tge(kk,:).*tm(kk).^3).^(1/4);

    syms XP
    CRm(kk,:) = (9/5) * (((1-sigma^2) .* a(kk,:).^2)./(16*pi*Yo.*tm(kk).^3));
    eqn = (3*XP./tge(kk,:)) - (5*pi.*a(kk,:).^2*Po.*CRm(kk,:)./tge(kk,:)) - 2*
        gFirstDerivativeFunc2(XP./tge(kk,:)).*(Vdc./Vr(kk,:)).^2 == 0;
%     XP_values(kk,:) = zeros(1,size(FpbOverFpg,2)); %dummy variable to keep
    values of XP
    for ii = 1:size(FpbOverFpg,2)
        ii
        XP_values(kk,ii) = solve(eqn(ii),'XP');
    end
%     XP = zeros(1,size(FpbOverFpg,2));
    XP = XP_values;

    A = (9/5)*ro*pi*(1-sigma^2)/(16*pi*Yo);
    B(kk,:) = eo*pi*gFunc2(XP(kk,:)./tge(kk,:));
    C(kk,:) = ((9*pi*(eo^2)*(Vdc^2)*(1-sigma^2))/(16*Yo)).*(
        gFirstDerivativeFunc2(XP(kk,:)./tge(kk,:))).^2;
    Ccolpitts = 5*10^-12; % C1=10p, C2=10p

%     sensitivity = zeros(1,size(FpbOverFpg,2));
%     mult = zeros(1,size(FpbOverFpg,2));
%     num1 = zeros(1,size(FpbOverFpg,2));
%     den1 = zeros(1,size(FpbOverFpg,2));
```

```
%      num2 = zeros(1,size(FpbOverFpg,2));
%      den2 = zeros(1,size(FpbOverFpg,2));
    for ii = 1:size(FpbOverFpg,2)
        mult(kk,ii) = (K1(kk,ii)*tm(kk)*(1-sigma^2))/(64*FpbOverFpg(ii)*pi*Yo);
        num1(kk,ii) = (-3*C(kk,ii)*(tm(kk)^(1/2))*(K1(kk,ii)^(3/2))*(tge(kk,ii)
            ^(-5/2)));
        den1(kk,ii) = ((A*tm(kk)*(K1(kk,ii))*(tge(kk,ii))*(B(kk,ii)*(tm(kk)
            ^(3/2))*(K1(kk,ii)^(1/2))*(tge(kk,ii)^(-1/2))+Ccolpitts))^(1/2)) *
            ((C(kk,ii)*(tm(kk)^(3/2))*(K1(kk,ii)^(3/2))*(tge(kk,ii)^(-5/2))+B(kk
            ,ii)*(tm(kk)^(3/2))*(K1(kk,ii)^(1/2))*(tge(kk,ii)^(-1/2))+Ccolpitts)
            ^(1/2));
        num2(kk,ii) = (-2*A*(K1(kk,ii))*(tge(kk,ii))*(B(kk,ii)*(tm(kk)^(3/2))*(
            K1(kk,ii)^(1/2))*(tge(kk,ii)^(-1/2))+Ccolpitts)) * ((C(kk,ii)*(tm(kk
            )^(3/2))*(K1(kk,ii)^(3/2))*(tge(kk,ii)^(-5/2))+B(kk,ii)*(tm(kk)
            ^(3/2))*(K1(kk,ii)^(1/2))*(tge(kk,ii)^(-1/2))+Ccolpitts)^(1/2));
        den2(kk,ii) = ((A*tm(kk)*(K1(kk,ii))*(tge(kk,ii))*(B(kk,ii)*(tm(kk)
            ^(3/2))*(K1(kk,ii)^(1/2))*(tge(kk,ii)^(-1/2))+Ccolpitts))^(3/2));
        sensitivity(kk,ii) = mult(kk,ii)*(num1(kk,ii)/den1(kk,ii) - num2(kk,ii)/
            den2(kk,ii));
    end

%      plot(FpbOverFpg,sensitivity(kk,:))
%      xlabel('FpbOverFpg');
%      ylabel('sensitivity');
%      title('sensitivity versus FpbOverFpg');
%      hold on

    %---------------------------------------------------------------
    %---------------------------------------------------------------

    Co(kk,:) = eo*(pi.*a(kk,:).^2)./tge(kk,:);
    LRm(kk,:) = ro*pi.*a(kk,:).^2.*tm(kk);

    nR(kk,:) = sqrt(5) .* (Co(kk,:)*Vdc./tge(kk,:)) .* gFirstDerivativeFunc2(XP(
        kk,:)./tge(kk,:));
    C0d(kk,:) = Co(kk,:) .* gFunc2(XP(kk,:)./tge(kk,:));
    CRS(kk,:) = (2.*tge(kk,:).^2)./(5.*Co(kk,:)*(Vdc^2).*gSecondDerivativeFunc2(
        XP(kk,:)./tge(kk,:)));

    K(kk,:) = 1./nR(kk,:);
    Ceq(kk,:) = (((-CRS(kk,:)).*CRm(kk,:))./(((-CRS(kk,:))+CRm(kk,:)))))./(K(kk
        ,:).^2);
    Leq(kk,:) = LRm(kk,:).*(K(kk,:).^2);
    fp(kk,:) = (1/(2*pi)).*(1./(sqrt(Leq(kk,:).*(C0d(kk,:).*Ceq(kk,:))./(C0d(kk
        ,:)+Ceq(kk,:)))));
    fs(kk,:) = (1/(2*pi)).*(1./(sqrt(Leq(kk,:).*Ceq(kk,:))));
    fo(kk,:) = (1/(2*pi)).*(sqrt((C0d(kk,:)+Ceq(kk,:)+Ccolpitts)./(Leq(kk,:).*
        Ceq(kk,:)*Ccolpitts+Leq(kk,:).*C0d(kk,:).*Ceq(kk,:)))); %resonant
        frequency
```

```
    c0 = 340; %speed of sound in air: 340m/s
    %Pressure(Po) = densityofAir(q0)*idealGasConstant(R)*Temperature(K)
    idealGasConstant = 287.058; %(287.058 J/(kg*K) %https://en.0wikipedia.org/index.php?q=aHR0cHM6Ly9lbi53aWtpcGVkaWEub3JnL3dpa2kvR2FzX2NvbnN0YW50)
    %q0 = 1.225; %At sea level and at 15 C air has a density of approximately 1.225 kg/m3 "https://en.wikipedia.org/wiki/Density_of_air"
    q0 = Po/(idealGasConstant*288);

    wavenumber(kk,:) = 2*pi.*fo(kk,:)/c0; %wavenumber at air
    ka(kk,:) = wavenumber(kk,:).*a(kk,:);

%      radiationImpedance = zeros(1,size(FpbOverFpg,2));
    for ii = 1:size(FpbOverFpg,2)
        radiationImpedance(kk,ii) = pi*(a(kk,ii)^2)*q0*c0*Z11_kaGreaterThan01(ka(kk,ii));
        if ka(kk,ii) < 0.1
            radiationImpedance(ii) = pi*(a(kk,ii)^2)*q0*c0*Z11_kaSmallerThan01(ka(kk,ii));
        end
    end

    Req(kk,:) = real(radiationImpedance(kk,:)).*(K(kk,:).^2);

    C1 = 10*10^-12; %10pF
    R1= 360000; %360K
    R2= 360000; %360K
    R3= 70000; %70K

    Qcmut(kk,:) = (2*pi.*fo(kk,:).*Leq(kk,:)./Req(kk,:));
    Zcmut(kk,:) = ((Req(kk,:) + (i*2*pi.*fo(kk,:).*Leq(kk,:)) + (1./(i*2*pi.*fo(kk,:).*Ceq(kk,:)))) .* (1./(i*2*pi.*fo(kk,:).*C0d(kk,:)))) ./ (Req(kk,:) + (i*2*pi.*fo(kk,:).*Leq(kk,:)) + (1./(i*2*pi.*fo(kk,:).*Ceq(kk,:))) + (1./(i*2*pi.*fo(kk,:).*C0d(kk,:))));
    Rcmut(kk,:) = real(Zcmut(kk,:));
    Lcmut(kk,:) = imag(Zcmut(kk,:))./(2*pi.*fo(kk,:));

    Rp(kk,:) = ((2*pi.*fo(kk,:)).^2.*(Lcmut(kk,:)).^2 + (Rcmut(kk,:)).^2)./Rcmut(kk,:);
    Lp(kk,:) = ((2*pi.*fo(kk,:)).^2.*(Lcmut(kk,:)).^2 + (Rcmut(kk,:)).^2)./((2*pi.*fo(kk,:)).^2.*(Lcmut(kk,:)));
    Rp2(kk,:) = (1+4*(2*pi.*fo(kk,:)).^2*C1^2*R3^2)./((2*pi.*fo(kk,:)).^2*C1^2*R3);
    Cp(kk,:) = (C1+2*(2*pi.*fo(kk,:)).^2*C1^3*R3^2)./(1+4*(2*pi.*fo(kk,:)).^2*C1^2*R3^2);
    Rparallel(kk,:) = ((1/R1)+(1/R2)+(1./Rp(kk,:))+(1./Rp2(kk,:))).^(-1);
    Qcircuit(kk,:) = Rparallel(kk,:).*(2*pi.*fo(kk,:)).*Cp(kk,:);
end

mycolours=jet(5);
for kk = 1:size(tm,2)
```

```
    plot(FpbOverFpg,sensitivity(kk,:),'color',mycolours(kk,:))
    xlabel('F_{pb}/F_{pg}');
    ylabel('sensitivity');
    title('sensitivity versus F_{pb}/F_{pg}');
    hold on
end
Legend=cell(size(tm,2),1);
 for iter=1:size(tm,2)
   Legend{iter}=strcat('tm = ', num2str(iter), ' um');
 end
 legend(Legend)

 figure
 mycolours=jet(5);
for kk = 1:size(tm,2)
    plot(FpbOverFpg,tge(kk,:)/10^-9,'color',mycolours(kk,:))
    xlabel('F_{pb}/F_{pg}');
    ylabel('t_{ge} (nm)');
    title('t_{ge} (nm) versus F_{pb}/F_{pg}');
    hold on
end
Legend=cell(size(tm,2),1);
 for iter=1:size(tm,2)
   Legend{iter}=strcat('tm = ', num2str(iter), ' um');
 end
 legend(Legend)

 figure
 mycolours=jet(5);
for kk = 1:size(tm,2)
    plot(FpbOverFpg,Rcmut(kk,:),'color',mycolours(kk,:))
    xlabel('F_{pb}/F_{pg}');
    ylabel('R_{CMUT} (ohm)');
    title('R_{CMUT} (ohm) versus F_{pb}/F_{pg}');
    hold on
end
Legend=cell(size(tm,2),1);
 for iter=1:size(tm,2)
   Legend{iter}=strcat('tm = ', num2str(iter), ' um');
 end
 legend(Legend)
```

A.2 gFunc2.m

```
function [ y ] = gFunc( u )
```

```
%This is the g(u) function
y = ((atanh(sqrt(u)))./(sqrt(u)));
end
```

A.3 gFirstDerivativeFunc2.m

```
function [ y ] = gFirstDerivativeFunc( u )
%This is the g'(u) function
y = ((1./(2.*u)) .* ((1./(1-u)) - ((atanh(sqrt(u)))./(sqrt(u)))));
end
```

A.4 gSecondDerivativeFunc2.m

```
function [ y ] = gSecondDerivativeFunc( u )
%This is the g''(u) function
y = (1./(2.*u)) .* ((1./((1-u).^2)) - 3.*gFirstDerivativeFunc2(u));
end
```